Journal of Hydrology xxx (2016) xxx–xxx

Contents lists available at ScienceDirect

Journal of Hydrology

journal homepage: www.elsevier.com/locate/jhydrol

Research papers

Development of a river-groundwater interaction model and its application to a catchment in Northwestern China

Litang Hu [a,*], Zongxue Xu [a], Weidong Huang [b]

[a] College of Water Sciences, Engineering Research Center of Groundwater Pollution Control and Remediation of Ministry of Education, Beijing Normal University, Beijing 100875, China
[b] Gansu Provincial Bureau of Hydrological and Water Resources Survey, Lanzhou, Gansu 730000, China

ARTICLE INFO

Article history:
Received 18 July 2016
Received in revised form 8 October 2016
Accepted 17 October 2016
Available online xxxx
This manuscript was handled by Corrado Corradini, Editor-in-Chief, with the assistance of Philip Brunner, Associate Editor

Keywords:
Surface water-groundwater interaction
Integrated numerical model
Arid regions
Heihe River Basin
Springs

ABSTRACT

The river-groundwater interaction is an important component of the hydrological cycle. This study develops an integrated river-GW model that uses a one-dimensional open channel flow model and a three-dimensional saturated GW flow model to describe the dynamic river-GW relationship at the basin scale, as well as groundwater flow and streamflow in arid regions. The model is tested with three cases, and the good agreement between the simulated and observed results demonstrates that the model can be used to simulate river-GW interactions. The integrated river-GW model is applied to the middle reaches of the Heihe River Basin and is calibrated using multi-source field data, including hydraulic heads from observation wells, streamflow, and spring flow. The case studies in the Heihe River Basin find that the following: (1) the river-GW relationships vary seasonally and spatially and depend on many factors, such as the river flow and GW uses; (2) in the middle reaches, the annual mean river–groundwater flux exchange from Yinluoxia to the Heihe Bridge is approximately 17% of the mean streamflow and increases to more than 49% from the Heihe Bridge to Zhengyixia; and (3) after the implementation of the water reallocation plan in 2000, the river-GW relationship in some reaches changed from a gaining stream to a losing stream due to the increase of GW abstraction. These findings suggest that GW pumpage should be controlled rationally and demonstrate that the integrated river-GW model can be used to analyse the temporal-spatial trends of river-groundwater interaction in arid regions.

1. Introduction

Surface water and groundwater are physically connected components of the hydrologic cycle (Winter et al., 1998). Surface water (SW)-groundwater (GW) interactions and their important influences on both SW and GW systems have been recognized by numerous researchers in the recent years (Winter, 1995; Sophocleous, 2002; Fernald and Guldan, 2006). For examples, lowering the water table has caused reductions in streamflow and drying of wetlands (Sophocleous, 2002; Chen et al., 2008; Brunner et al., 2009), and reductions of streamflow have caused decline of the groundwater table and decrease of groundwater pumpage in the near-river regions (Wang et al., 2011). Understanding the interactions between SW and GW is critical to effectively utilize water resources, avoid conflicts of water use between adjacent provinces and to maintain ecosystem diversity and functioning (Winter, 1995; Sophocleous, 2002; Malcolm et al., 2003). Up to now, SW-GW interactions have been investigated extensively (Winter, 1995; Pucci and Pope, 1995; Winter et al., 1998; Ojiambo et al., 2001; Sophocleous, 2002; Malcolm et al., 2003; Miller et al., 2003; Lamontagne et al., 2005; Fernald and Guldan, 2006; Harvey et al., 2006; Chen et al., 2008; Furman, 2008; Brunner et al., 2009; Irvine et al., 2012; Partington et al., 2012). SW-GW flux exchanges and relationships are important topics. Three main methods can be used to investigate SW-GW interactions. The first is a statistical analysis based on monitoring data of GW levels and streamflow (Newman et al., 2006; Woocay and Walton, 2008; Ward et al., 2013). Another important technique is the analysis of environmental isotopes and geologic, hydrochemical and in situ physicochemical parameters (Katz et al., 1997; Ojiambo et al., 2001; Lamontagne et al., 2005; Lang et al., 2006; Kumar et al., 2008). A common method is numerical model to quantify the flux between SW and GW (Pucci and Pope, 1995; Yu and Schwartz, 1998; Miller et al., 2003; Werner et al., 2006; Harvey et al., 2006; Velazquez et al., 2008; Yuan and Lin, 2009; Zaadnoordijk, 2009; Wu et al., 2014; Zhu et al., 2014; Zhang and Liu, 2015). Integrated SW-GW simulators, such as InHM (Abel et al., 2008), MODHMS (Panday and Huyakorn, 2004), MIKE SHE

* Corresponding author.
E-mail addresses: litanghu@bnu.edu.cn (L. Hu), zongxuexu@vip.sina.com (Z. Xu), gsdxhwd@163.com (W. Huang).

http://dx.doi.org/10.1016/j.jhydrol.2016.10.028
0022-1694/

(Refsgaard, 1997), HydroGeosphere (Therrien et al., 2007), and GSFLOW (Markstrom et al., 2008), are usually used in the management of SW-GW resources.

The Heihe River Basin (HRB), located in the middle part of the Hexi Corridor, is the second largest inland river in China and has a total length of approximately 928 km (Fig. 1a). The river originates from a glacier in the Qilian Mountains and flows northeast across the middle reaches of the HRB. As part of an old silk road, the HRB has experienced rapid societal and economic development and a rapid increase in the population density. The middle reaches of the main stream of the Heihe River are areas of grain production and have a well-developed irrigation system. Excessive abstraction of groundwater in the middle reaches over the past 30 years has caused a continuous decline of the GW level, which has significantly affected the streamflow of the Heihe River and has resulted in the disappearance of large areas of wetlands in the downstream regions (Hui et al., 2005). The optimized use of surface water and GW in the HRB is important for the sustainable development of the ecosystem and economics. The HRB flows across Qinghai Province (the upper reach), Gansu Province (the middle reach) and the Inner Mongolia Autonomous Region (the lower reach). There is a serious conflict of water uses between the upper and lower reaches, which dates back to 1726 CE of the Qing dynasty (Zhong, 1995). Numerous studies have examined the conflicts of interests in the allocation of water resources, and several measures have been proposed to address this issue (X.J. Wang et al., 2015; Z.J. Wang et al., 2015). The water resources reallocation plan in the HRB was initiated in 1992 and was implemented in 2000 by the Chinese central government. Under the financial support of a major research plan of the National Natural Science Foundation of China (NSFC), the HRB was selected as a typical arid inland region to carry out integrated and multidisciplinary basin-scale studies on field observations, sustainable water resource management, and the relationships between water, ecology, economics and society (Cheng et al., 2014). Among the HRB researches, the river-GW interaction is one of the most important topics.

Recently, the interaction between river and GW in the HRB has gained increasing amounts of attention. Most researches (Lan et al., 2002; Cheng et al., 2014; Nian et al., 2014; X.J. Wu et al., 2015; Deng and Zhao, 2015) were focused on the budgets of groundwater components, and rational use of water resources under different land uses using the hydrologic observation data. A coupled river-GW model is necessary to systematically understand the river-GW relationship to efficiently manage water resources in the HRB due to recent human activities. The existing groundwater models in the HRB are limited and can be classified into three types: (1) GW model without SW model (Hu et al., 2007); (2) GW model with rule-based lumped SW model (Hu et al., 2009; Wang et al., 2010); (3) coupled river-GW model (Jia et al., 2009; Tian et al., 2015a, 2015b; Yao et al., 2015a, 2015b; B. Wu et al., 2015). Because the surface and subsurface systems follow different partial differential equations, the coupling of river and GW domain is of great importance to accurately address water resources problems in the HRB. Coupling of river-GW model is difficult, however, coupled river-GW model is efficient because processes in both groundwater flow and streamflow are represented. The WEP-Heihe model (Jia et al., 2009) is a distributed hydrological model but its treatment of the groundwater component was too simplistic to represent the groundwater flow characteristics in the middle reaches of the HRB. Other researchers have used the GSFLOW model in the HRB (Tian et al., 2015a, 2015b; Yao et al., 2015a, 2015b). They concluded that developing regional groundwater models with high spatial and temporal resolutions is urgently needed for water resources management in the HRB (Yao et al., 2015a, 2015b). They also found that significant river-GW interaction mainly occurs in the main stream of the HRB, and river-GW exchange has notable spatial and temporal variations. Hu et al. (2007) simulated the interactions between rivers, springs and GW in the HRB using a numerical GW flow model, but did not represent the process of streamflow. Up to now, the interactions between the main stream of the Heihe River, spring flow and GW, and especially how the relationship between the Heihe River and GW has evolved due to human activities in recent years, are still not well understood. Physically-based coupled river-GW models provide comprehensive tools for analysing groundwater level changes, flux exchanges of river and groundwater. However, most models cannot present clearly how river-groundwater relationship changes at the spatial and temporal scales. Also, complex coupled SW-GW models, such as InHM and MIKE-SHE, are not applicable at the basin scale because the model setup needs a lot of data input. To sum up, it is still of importance to develop coupled river-GW model in arid regions to integrate field observations and provide a detailed temporal-spatial demonstration of the hydrological cycle in the HRB.

The objective of this paper is to develop an integrated river-GW flow model to analyse the temporal-spatial evolution of the Heihe River-GW interaction from 1995 to 2014 in the middle reaches of the HRB using up-to-date field observation data. First, an integrated river-GW flow model (denoted river-GW model) is developed to identify the river-GW interaction. The river-GW model is then tested using the following three test cases: (i) the problem of a continuous point sink in a homogeneous aquifer; (ii) the channel flow problem of the Sacramento River, and (iii) a hypothetical case of river-GW interaction. Second, a river-GW model of the middle reaches of the HRB is developed. Third, the model is calibrated and validated using field observation data from 1995 to 2014, including observation well data, streamflow in the Heihe River and spring flow. Finally, the temporal-spatial changes of the Heihe River-GW interaction will be discussed in detail.

2. Numerical code development

The framework of the river-GW model is shown in Fig. 2. The model includes flow models of SW and saturated GW. A time step of the saturated GW flow model may include one or more time steps of the SW model (Fig. 2a). The spatial discretization of the river network is the same as that of the GW grid system (Fig. 2b). To describe the river-GW relationship and calculate the river-groundwater flux exchanges, the river stages are usually given as prescribed values in the traditional GW model. However, the coupled river-GW model can easily simulate the river stage and streamflow at each time step for each discretized grid cell using the open channel flow model. Furman (2008) classified the coupling into three types: uncoupled (externally coupling), iterative coupling, and fully coupled. Considering numerical difficulties in solving governing equations and boundary conditions in SW and GW domain simultaneously (fully coupled), externally coupled method at each time step is used in developed model. In SW sub-model, water table for each discretized grid cell is given explicitly as that in the former time step. In the GW sub-model, the simulated river stage from SW sub-model is then used to calculate hydraulic head and the river–groundwater flux exchange.

2.1. Surface water flow model

In the middle and lower reaches of river basin of most arid regions, the processes of precipitation–runoff are not significant, however, water consumption and streamflow are dominant hydrology processes. So a river in the SW flow model is represented as an open channel to simulate the change of streamflow. According to the principles of water continuity and

Please cite this article in press as: Hu, L., et al. Development of a river-groundwater interaction model and its application to a catchment in Northwestern China. J. Hydrol. (2016), http://dx.doi.org/10.1016/j.jhydrol.2016.10.028

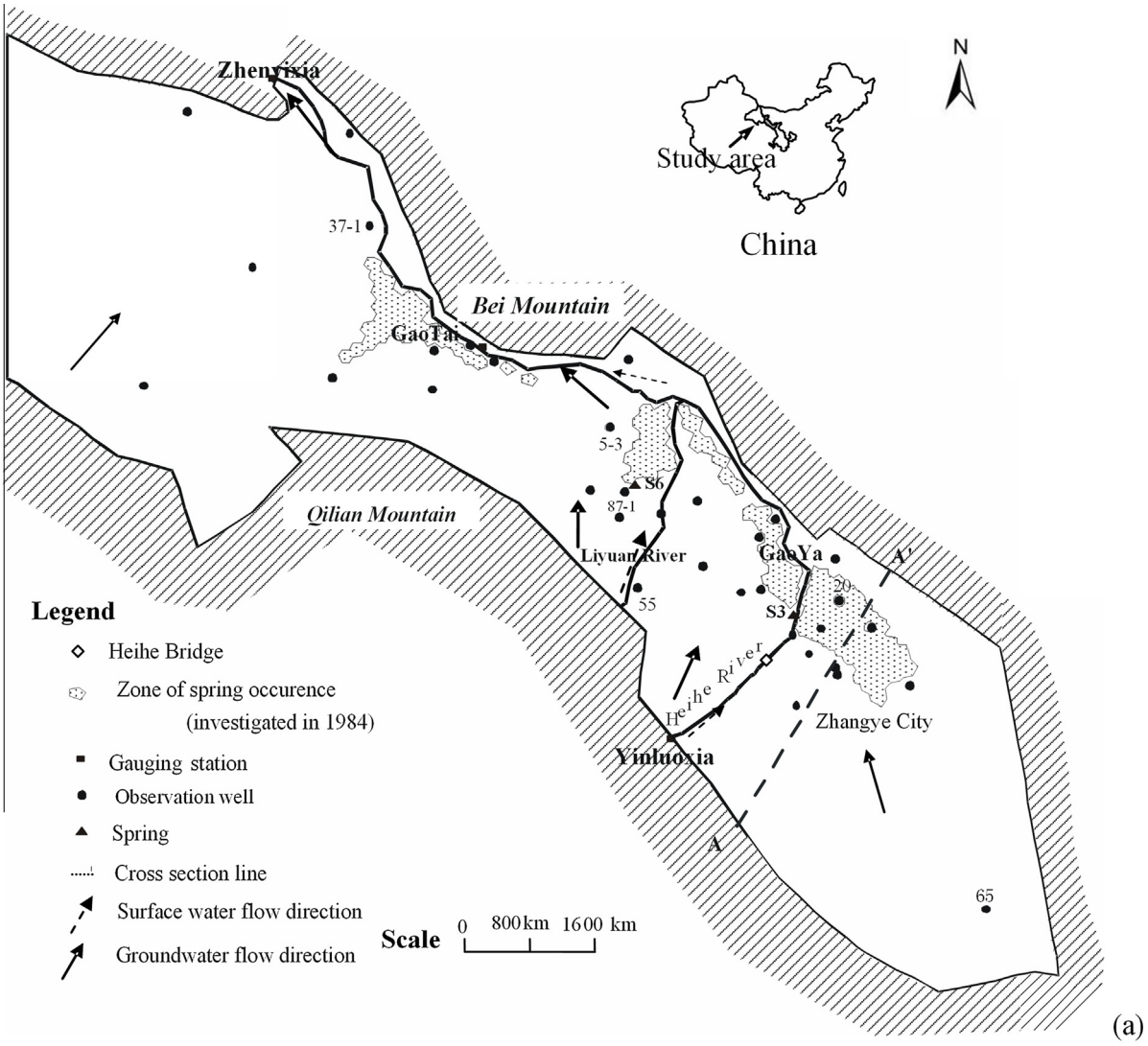

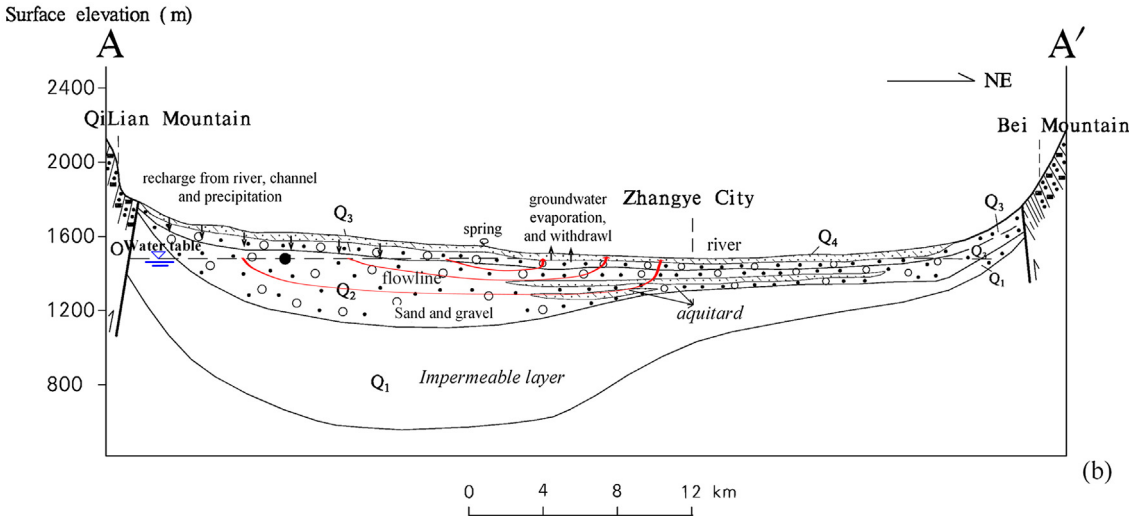

Fig. 1. Schematic map of the study area. (a) Plain view and (b) schematic hydrogeological cross-section along AA′.

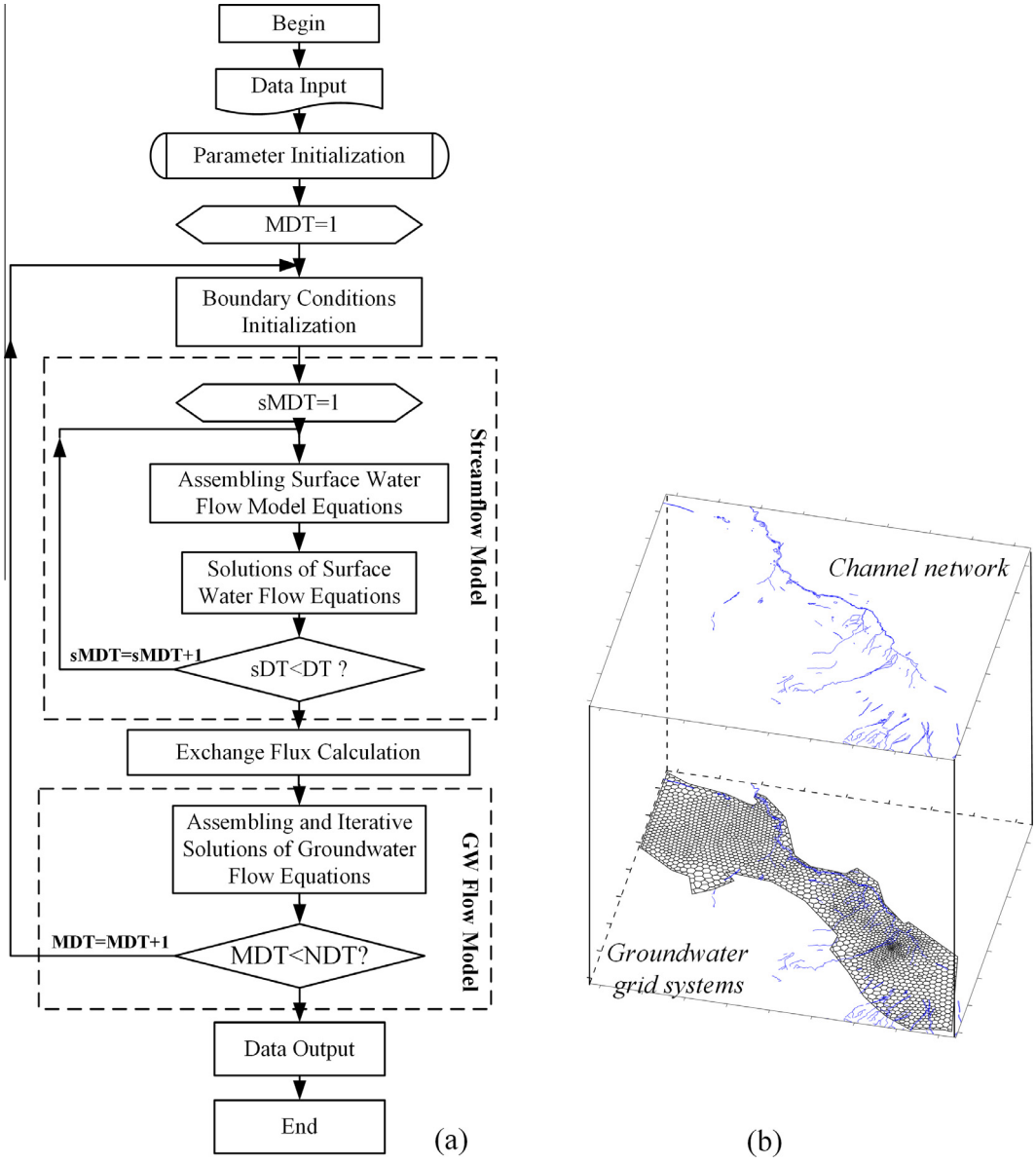

Fig. 2. Framework and grid system of the integrated river-GW model. (a) Framework and (b) grid system. (Notation: MDT is the time step index in the GW model; DT is the time step of the GW model; sMDT is the time step index of the SW model; sDT is the time step of the SW model; NDT indicates the total number of time steps; SW is surface water; GW is groundwater.)

momentum conservation, the governing equations of the open channel flow model (Schaffranek et al., 1981) are given in Eqs. (1) and (2).

$$\begin{cases} B\frac{\partial Z}{\partial t}+\frac{\partial Q}{\partial x}+q-q_s=0 \\ \frac{1}{gA}\cdot\frac{\partial Q}{\partial t}+\frac{2\beta Q}{gA^2}\cdot\frac{\partial Q}{\partial x}-\frac{\beta Q^2}{gA^3}\cdot\frac{\partial A}{\partial x}+\frac{\partial Z}{\partial x}+\frac{k}{A^2R^{4/3}}Q\cdot|Q|-\frac{\xi B}{gA}\cdot U_a^2\cos\varphi=0 \end{cases} \quad (1)$$

$$q=K'\mathrm{B}(\mathrm{Z}-\mathrm{h})/b' \quad (2)$$

where B is the river width (L); Z is the river stage (L); Q is the flow rate of the river (L^3/T); x is the longitudinal distance down the river (L); q is the flux exchange between the river and the GW (L^2/T); q_s is the outflow per unit length of the channel (L^2/T); K' is the hydraulic conductivity of the riverbed (L/T); b' is the thickness of the riverbed (L); h is the hydraulic head (L); g is the gravitational acceleration (L/T^2); A is the cross-sectional area of the river (L^2); β is the momentum coefficient (dimensionless); k is the friction factor based on Manning's equation (dimensionless); R is the hydraulic radius (L); ξ is a coefficient (dimensionless) that is equivalent to $C_d\rho_a/\rho_w$, where ρ_a is the density of air (M/L^3), ρ_w is the density of water (M/L^3), and C_d is the water surface drag coefficient (dimensionless); U_a is the wind speed (L/T); and φ is the angle between the wind and the river's orientation (radian).

The rivers are discretized into a series of grid cells along the river channel. Every pair of adjacent grid cells follows Eq. (1). All of the equations, with the initial river stage and streamflow data and the boundary conditions, are solved using the Successive Over-Relaxation (SOR) method. The formulation of the equations is the same as in the FORTRAN codes of the BRANCH model (Schaffranek et al., 1981; Swain and Wexler, 1996).

Please cite this article in press as: Hu, L., et al. Development of a river-groundwater interaction model and its application to a catchment in Northwestern China. J. Hydrol. (2016), http://dx.doi.org/10.1016/j.jhydrol.2016.10.028

2.2. Groundwater flow model

The governing equation for GW flow is given in Eq. (3).

$$\begin{cases} \frac{\partial}{\partial x}\left(Kh\frac{\partial H}{\partial x}\right)+\frac{\partial}{\partial y}\left(Kh\frac{\partial H}{\partial y}\right)+\frac{\partial}{\partial z}\left(Kz\frac{\partial H}{\partial z}\right)+w=S_s\frac{\partial H}{\partial t}(x,y,z)\in D,\ t>0 \\ H|_{t=0}=H_0(x,y,z)(x,y,z)\in D,\ t>0 \\ H(x,y,z,t)|_{(x,y,z)\in B_1}=H_1(x,y,z,t),\ t>0 \\ -T\frac{\partial H}{\partial n}|_{(x,y,z)\in B_2}=q_2,\ t>0 \end{cases} \tag{3}$$

where H is the hydraulic head (L); x, y, z are the coordinates in the x, y, and z directions, respectively (L); K_h and K_z are the horizontal and vertical hydraulic conductivities, respectively (L/T); w is the volumetric flux per unit of the representative sources and sinks of water (1/T); S_s is the specific storage (1/L); H_0 is the initial hydraulic head (L); H_1 is the hydraulic head at the Dirichlet-type boundary (L); T and q_2 are the transmissivity and flux at the Neumann-type boundary, respectively (L^2/T); B_1 is the Dirichlet-type boundary; B_2 is the Neumann-type boundary; D is the modelled area; and t is time (T).

The modelled area is discretized into a series of hexahedral or wedge-shaped grids and a triangular mesh in an assistant network (Chen et al., 2003; Hu et al., 2007). When considering the water balance zone around one grid cell, according to Darcy's law and the principle of water continuity, the change in GW storage at that grid cell is the sum of the lateral and vertical flows and the GW sources and sinks (e.g., pumping rate, spring flux, discharge to rivers, infiltration). A finite difference method for polygonal grid cells (Chen et al., 2003, 2014; Hu et al., 2007) is used to solve the numerical GW flow model. The difference equation can be written as Eq. (4) (Hu et al., 2007; Chen et al., 2014). The equations are solved using the Successive Over-Relaxation (SOR) method.

$$\begin{aligned} &\sum_e\left[T_{ij}\frac{\overline{pb}}{\overline{ij}}h_j^{n+1}+T_{ik}\frac{\overline{bq}}{\overline{ik}}h_k^{n+1}\right]+\left[\frac{K_{ii'}}{Z_{i'}-Z_i}h_{i'}^{n+1}+\frac{K_{ii''}}{Z_i-Z_{i''}}h_{i''}^{n+1}\right]A_i \\ &-\left[\sum_e\left(T_{ij}\frac{\overline{pb}}{\overline{ij}}+T_{ik}\frac{\overline{bq}}{\overline{ik}}\right)+\left(\frac{K_{ii'}}{Z_{i'}-Z_i}+\frac{K_{ii''}}{Z_i-Z_{i''}}\right)A_i+S_{si}\frac{A_i}{\Delta t}\right]h_i^{n+1} \\ &=-S_{si}\frac{h_i^n}{\Delta t}A_i-Q_{wi} \end{aligned} \tag{4}$$

where e is the area over which the water balance equation is written; $\underline{Tij}$ and T_{ik} are the mean transmissivities of lines ij and ik, respectively (L^2/T); $\overline{ij}, \overline{pb}, \overline{ik}, \overline{bq}$ are the lengths of lines ij, pb, ik and

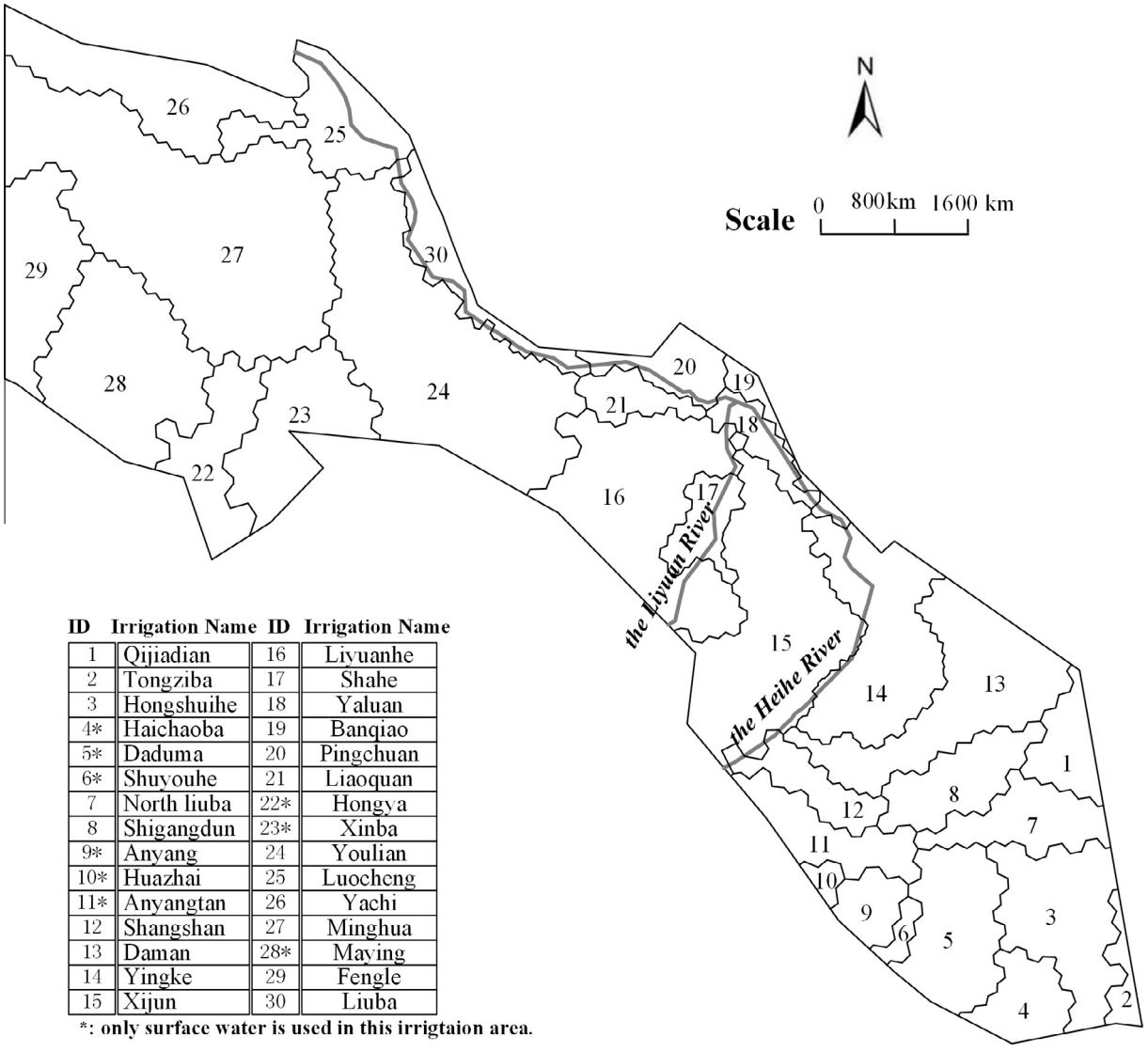

ID	Irrigation Name	ID	Irrigation Name
1	Qijiadian	16	Liyuanhe
2	Tongziba	17	Shahe
3	Hongshuihe	18	Yaluan
4*	Haichaoba	19	Banqiao
5*	Daduma	20	Pingchuan
6*	Shuyouhe	21	Liaoquan
7	North liuba	22*	Hongya
8	Shigangdun	23*	Xinba
9*	Anyang	24	Youlian
10*	Huazhai	25	Luocheng
11*	Anyangtan	26	Yachi
12	Shangshan	27	Minghua
13	Daman	28*	Maying
14	Yingke	29	Fengle
15	Xijun	30	Liuba

*: only surface water is used in this irrigtaion area.

Fig. 3. Locations of irrigation areas.

Please cite this article in press as: Hu, L., et al. Development of a river-groundwater interaction model and its application to a catchment in Northwestern China. J. Hydrol. (2016), http://dx.doi.org/10.1016/j.jhydrol.2016.10.028

bq, respectively (L); $K_{ii'}$ and $K_{ii''}$ are the vertical hydraulic conductivities at grid cell i in layers $s-1$ and $s+1$, respectively (L/T); h_i, h_j, h_k are the mean GW heads of grid cells i, j, and k, respectively (L) in layer s; $Z_i, Z_{i'}, Z_{i''}$ are the elevations of grid cell i in layer s, the upper layer and the lower layer, respectively (L); A_i is the area controlled by grid cell i (L^2); S_{si} is the specific storage of grid cell i (1/L); Δt is the time step of the GW model (T); Q_{wi} is the flow rate, including infiltration, GW evaporation, and the pumping rate, at grid cell i (L^3/T); and n is the serial number of the time step.

The integrated model is tested with three test cases, including the problem of a continuous point sink in a homogeneous aquifer, the channel flow problem of the Sacramento River and the river-GW relationship induced by GW pumping. The test cases are described in Appendix A. The IGMESH (Hu et al., 2016), SURFER and ARCGIS software are used to perform the modelling analysis. Unlike statistical analysis, physically based river-GW model follows the physics law of water movement, and its application need a lot of data input. At the basin scale, many experiments and investigations are needed to obtain these data. To avoid over parameterization, the parameter estimations in the case study are almost based on the field tests and hydrogeological investigation so as to keep the proper number of the zonation of parameters.

3. Conceptual model and data collection

3.1. Study area description

The study area is a sedimentary basin that covers an area of approximately 8700 km^2, which is surrounded by the Qilian Mountains to the south, the Bei Mountains to the north and is adjacent to another basin to the east (Fig. 1a). The surface elevation ranges from 2200 m in the south to 1290 m in the north. The HRB mainly includes the main Heihe River, the Liyuan River, and the following three hydrological stations that are located in the basin: Yiluoxia, Gaoya, and Zhengyixia. The Heihe River turns from Yiluoxia to the northwest at Zhangye City and flows into the downstream delta oasis at Zhengyixia (Fig. 1a). The annual mean streamflow of the Heihe River at Yiluoxia is 1.58 billion m^3, and the annual mean streamflow of the Liyuan River is 0.22 billion m^3. The GW generally flows from southwest to northeast. Data from 101 boreholes were collected from the study area, and a simplified hydrogeologic cross-section (Hydrogeoglogical Team and Hydrology and Water Resources Units of Zhangye in Gansu Province, 1990) is shown in Fig. 1b. The aquifers mainly consist of porous Quaternary deposits. In the high southern part of the study area, the aquifer is composed of thick uniform sand with good permeability (hydraulic conductivity may be over 50 m/d). In the lower northern part, the lithology changes to thin layers of fine sand and clay. Thus, the aquifer varies from a uniform layer to multiple layers from south to north.

The interrelation between river and GW in the region is a typical characteristic of the northwest arid region of China. As shown in Fig. 1b, the GW is fed by river leakage in the upper part of the alluvial fans and then discharges in the form of spring flow or directly into the Heihe River near the edge of the fans because the sediments gradually become finer, and the hydraulic conductivity decreases. The GW is also recharged from the infiltration of irrigation water. When a river incises aquifers and is lower than the GW head, the river becomes a natural channel for GW dis-

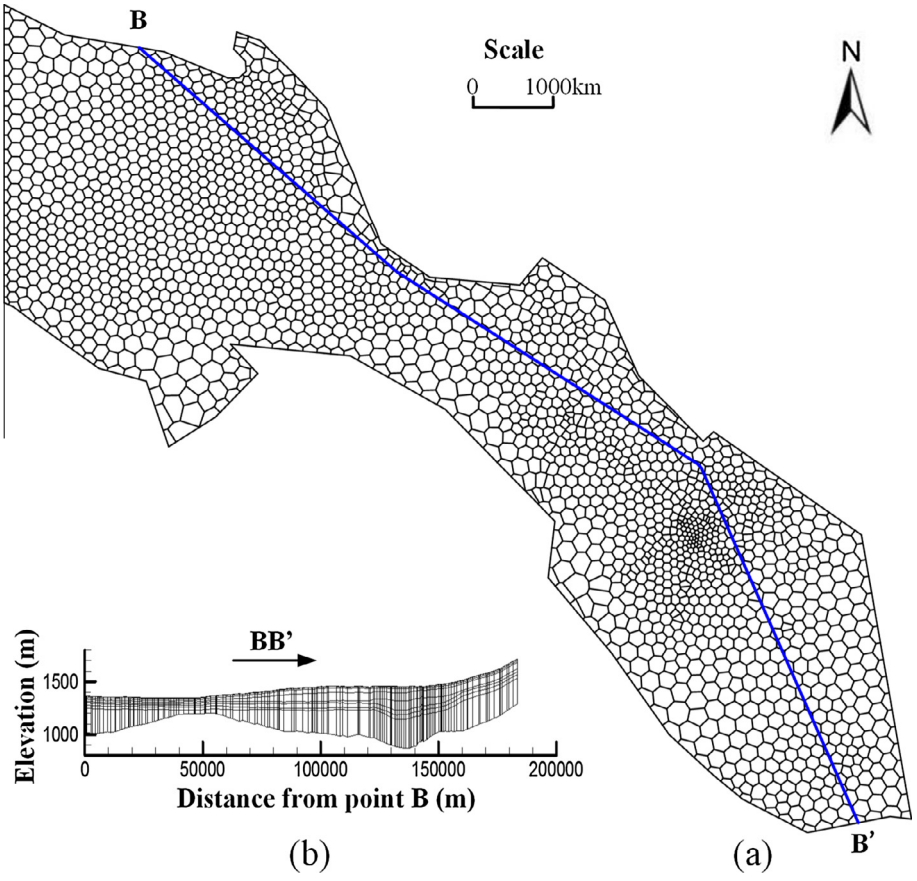

Fig. 4. Schematic illustrations of the grid system and a typical cross-section across the HRB. (a) Grid system and (b) cross-section.

charge. Springs, river discharge, evaporation from shallow GW and human exploitation are the main components of the GW discharge, of which springs and river discharge make up approximately 65% (Hydrogeoglogical Team and Hydrology and Water Resources Units of Zhangye in Gansu Province, 1990). The annual mean leakage from rivers, channels and return flow of irrigation water is the main source of recharge to the GW and accounts for 80% of the total recharge (Hydrogeoglogical Team and Hydrology and Water Resources Units of Zhangye in Gansu Province, 1990).

3.2. Conceptual model of the integrated system

The model is chosen to coincide with the area of the middle reaches of the HRB. The Heihe River is set as an open channel because abundant gauging data are available. The river stage and flux at Yinluoxia are assumed as boundary conditions with known values. The southwestern boundary of the saturated GW flow system is represented by a flux boundary, and the northeastern boundary is set as a no-flow boundary. The flux at the southwestern boundary is obtained from hydrogeological investigation carried out by Hydrogeoglogical Team and Hydrology and Water Resources Units of Zhangye in Gansu Province in 2002. The western boundary is extended to the water divide between the HRB and the adjoining basin and is represented by a no-flow boundary. The upper boundary includes infiltration from rainfall, the Heihe River and channels, irrigation return flows in irrigated areas, and GW evaporation. The consolidated Quaternary sediments are treated as the bottom no-flow boundary. The thickness of the aquifer ranges from 50 to 800 m but is between 100 and 300 m in most of the area. In the southern part of the model area, the aquifer system is represented by a relatively thick and homogeneous sandy layer. The lithology can be classified into clay, loose sand with gravel, fine-grained sand, and weathered granite, and these units are interbedded in the northern part of the study area. A maximum of 8 aquifers and aquitards are present. The numerical method of describing the Heihe River-GW relationship and spring flow is the same as in previous studies (Hu et al., 2007). The river-GW relationship is determined automatically in the model based on the river stage, the GW level and the elevation of the semipermeable media at the base. The spring flow is calculated from the elevation, hydraulic conductivity, contact area and thickness of the aquifer, and the hydraulic head at the location of the spring. Unsaturated flow is very important in areas with a large depth to groundwater. For compensating the shortage of unsaturated flow in developed river-GW model, effect of hysteresis on infiltration

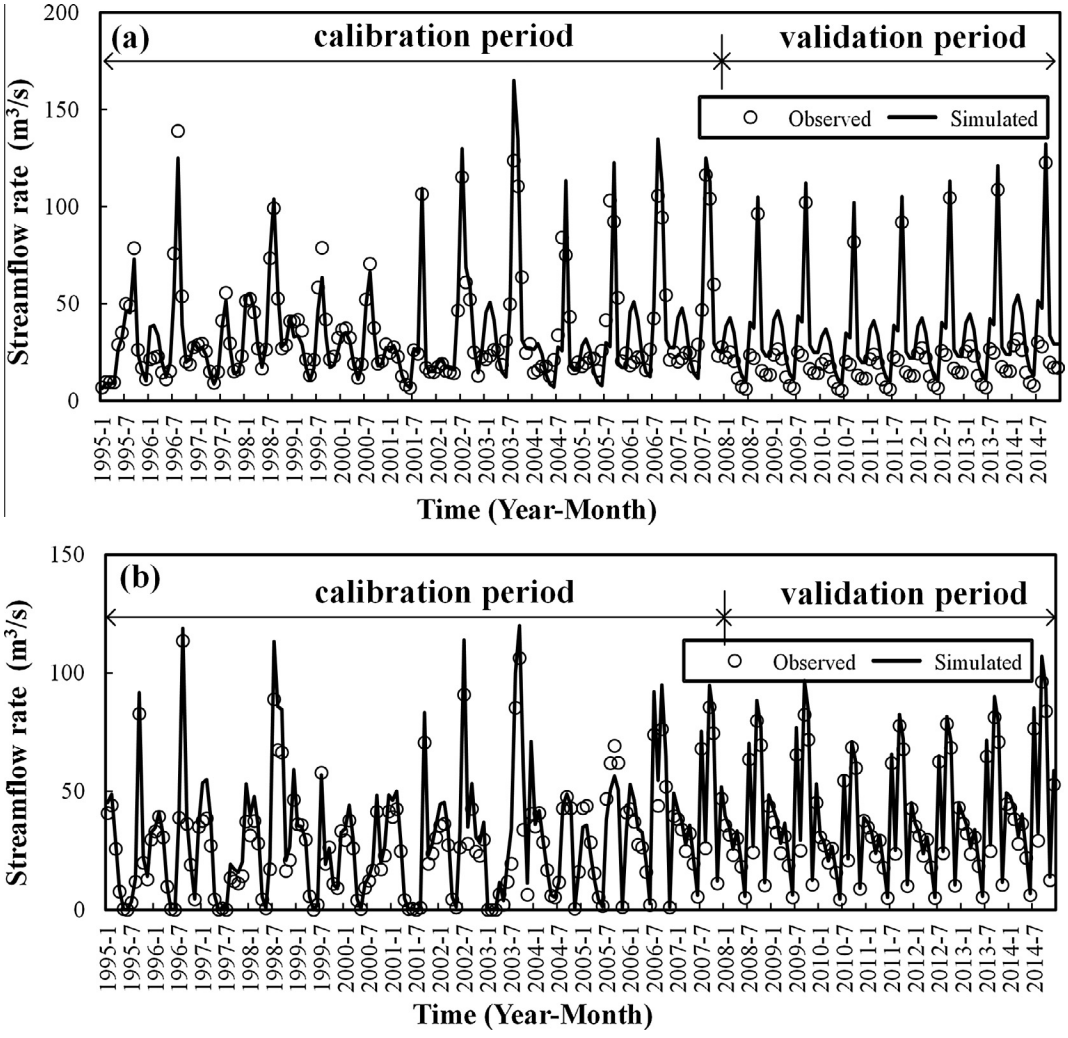

Fig. 5. Comparison of observed and simulated streamflow of the Heihe River at Gaoya (a) and Zhengyixia (b) for the calibration and validation period.

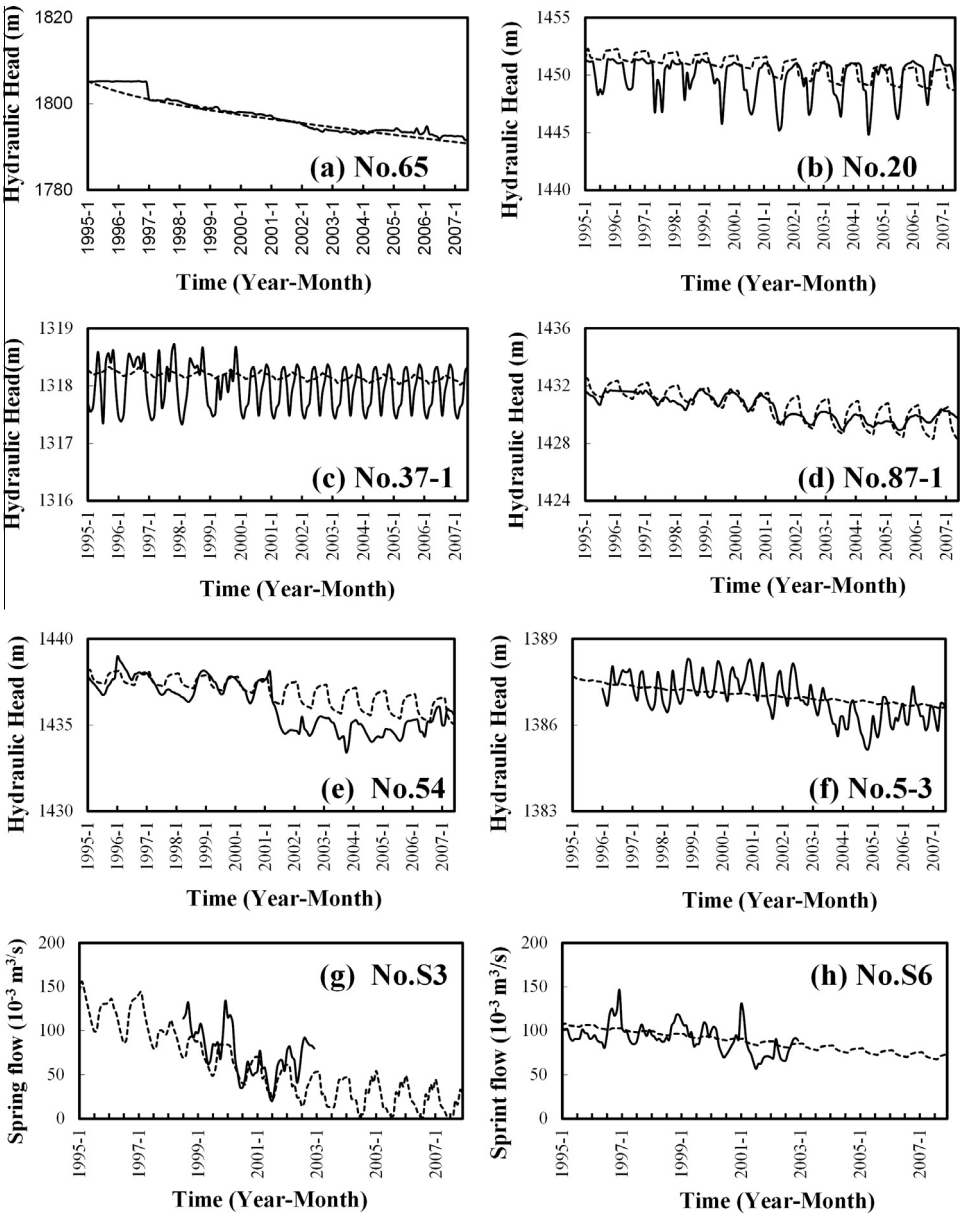

Fig. 6. Comparison of simulated and observed hydraulic heads at six observation wells (a–f) and springs flows at two monitoring sites (g and h) for the calibration period. (Dash and solid lines represent simulated and observed values, respectively.)

Table 1
Statistics of the absolute errors in the simulated GW levels.

Errors (m)	$\Delta H \leqslant 0.2$	$0.2 < \Delta H \leqslant 0.5$	$0.5 < \Delta H \leqslant 1.0$	$1.0 < \Delta H \leqslant 1.2$	>1.2	Total
No. of readings	1065	1370	1148	215	1574	5372
Percentage	19.83	25.50	21.37	4.00	29.30	100

Table 2
Model efficiency evaluation.

Targets	Period	Nash-Sutcliffe efficiency	
		Gaoya station	Zhengyixia station
Runoff	Calibration	0.74	0.9
	Verification	0.75	0.96
Hydraulic head	Calibration	0.99	
Spring flow	Calibration	0.21	

rate from rainfall and return flow of irrigations through a thick vadose zone is characterized using a weight function method (Chen, 1998). It is also noted that multiaquifer observation wells (Neville and Tonkin, 2004) are generally present in the HRB, and the coupled seepage-pipe flow is used to simulate the flow in multiaquifer wells (Hu et al., 2007).

3.3. Data preparation

3.3.1. Precipitation and evaporation

The study area has a typical arid continental climate with an annual mean precipitation of 129 mm and an annual mean potential evaporation of 2048 mm. Mean precipitation data of the study area from 1995 to 2014 were available for this study. Overall, the precipitation increased from 2000 to 2014. The mean yearly pre-

cipitation ranged from 70 mm to 214 mm. During each year, the maximum and minimum precipitation occurs from June to August and from November to January of next year, respectively. The precipitation decreases from south to north. According to Hydrogeoglogical Team and Hydrology and Water Resources Units of Zhangye in Gansu Province (1996), the infiltration coefficient of precipitation, which is the ratio of the infiltration rate to the precipitation rate (dimensionless), ranges from 0.01 in the south to 0.31 in the north.

GW evaporation depends mainly on the climate, soil structure and potential evapotranspiration. According to soil lysimeter tests (Hydrogeoglogical Team and Hydrology and Water Resources Units of Zhangye in Gansu Province, 1996), GW evaporation may be calculated from Eq. (5)

$$\varepsilon_{gw} = \varepsilon_0 \cdot \exp(-b \cdot D_g) \quad (5)$$

where D_g is the depth to GW (L); ε_0 is the potential evapotranspiration (L); and b is an empirical coefficient, which is estimated from soil lysimeter tests (set to 0.9858 in the model; L^{-1}).

3.3.2. River stage and streamflow data

The Heihe River is assumed to have a uniform width and cross-sectional area because geometry of the Heihe River is not measured over the regional scale. The annual streamflow at Yiluoxia and Zhengyixia from 1995 to 2014 have similar increasing trends. The river stage at Yiluoxia is set to known boundary values, which are the statistics of the Zhangye Provincial Bureau of Hydrological and Water Resources Survey.

3.3.3. Irrigation area and water uses

The study area contains 30 irrigation areas (Fig. 3). GW receives recharge from infiltration from canals and return flow of irrigation water. In some areas near the Liyuan and Heihe rivers, GW is recharged from the rivers. According to previous studies (Hydrogeoglogical Team and Hydrology and Water Resources Units of Zhangye in Gansu Province, 1996), the infiltration from canals is approximately 4.5×10^8 m^3/a, and the return flow is approximately 2.5×10^8 m^3/a. Nine of the 30 irrigation areas use SW (Fig. 3), while the others utilize GW.

GW pumpage in the irrigation areas differed before and after 2000. Before 2000, most of the GW was pumped in the Daman, Yingke and Youlian irrigation areas (approximately 0.5×10^8 m^3/a). After 2000, which was the beginning of the water reallocation plan of the HRB, GW pumping in the Daman and Yingke irrigation areas increased to more than 1.1×10^8 m^3/a and that in the Youlian irrigation area decreased to approximately 0.08×10^8 m^3/a. GW withdrawals in the other irrigation areas also increased. Overall, the GW withdrawals increased from approximately 2.5×10^8 m^3 in 1995 to more than 4.5×10^8 m^3 in 2014.

3.3.4. Hydraulic head and springs flow data

The study area contains 34 observation wells, which cover the different depths of the aquifer. In the southern part of the study area, the GW level decreased continuously with a maximum rate of more than 1.0 m per year. In the northern part near the Heihe River, the GW level has been almost constant with annual fluctuations of only 0.5 m. The hydraulic head varies with depth in the aquifer, even at the same location. There is approximately 1 m vertical hydraulic head difference measured in well No. 5.3.

Springs are important discharge components of the GW system. Long-term observation data are available for two springs (S3 and S6; Fig. 2a). S3 is located near the Heihe River, and its discharge decreased notably from approximately 0.14 m^3/s in 1999 to 0.08 m^3/s in 2003. S6 is located near the Liyuan River, and the flow decreased from approximately 0.13 m^3/s in 1995 to approximately 0.08 m^3/s in 2003. It is worth noting that there are many other springs without observation data, which converge into the main reaches of the Heihe River. According to an investigation by the

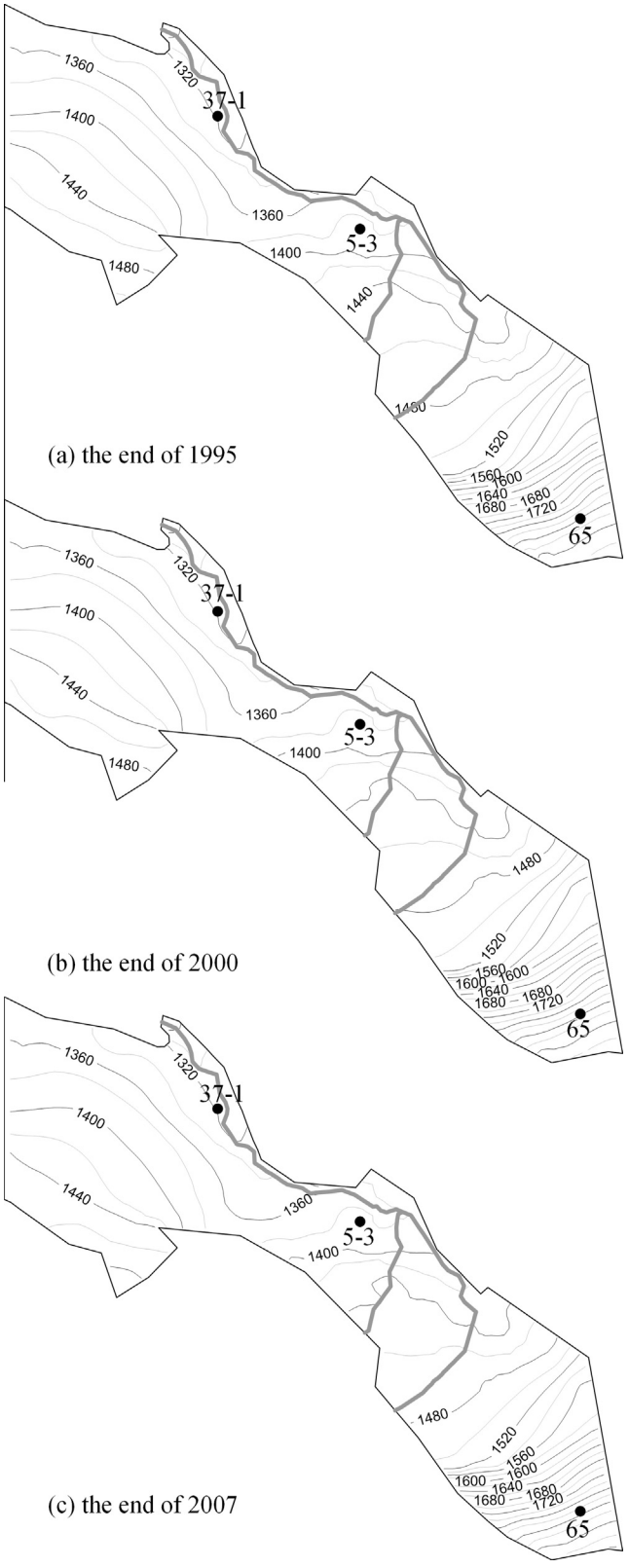

Fig. 7. Contour maps of the water table at the ends of 1995 (a), 2000 (b) and 2007 (c).

Please cite this article in press as: Hu, L., et al. Development of a river-groundwater interaction model and its application to a catchment in Northwestern China. J. Hydrol. (2016), http://dx.doi.org/10.1016/j.jhydrol.2016.10.028

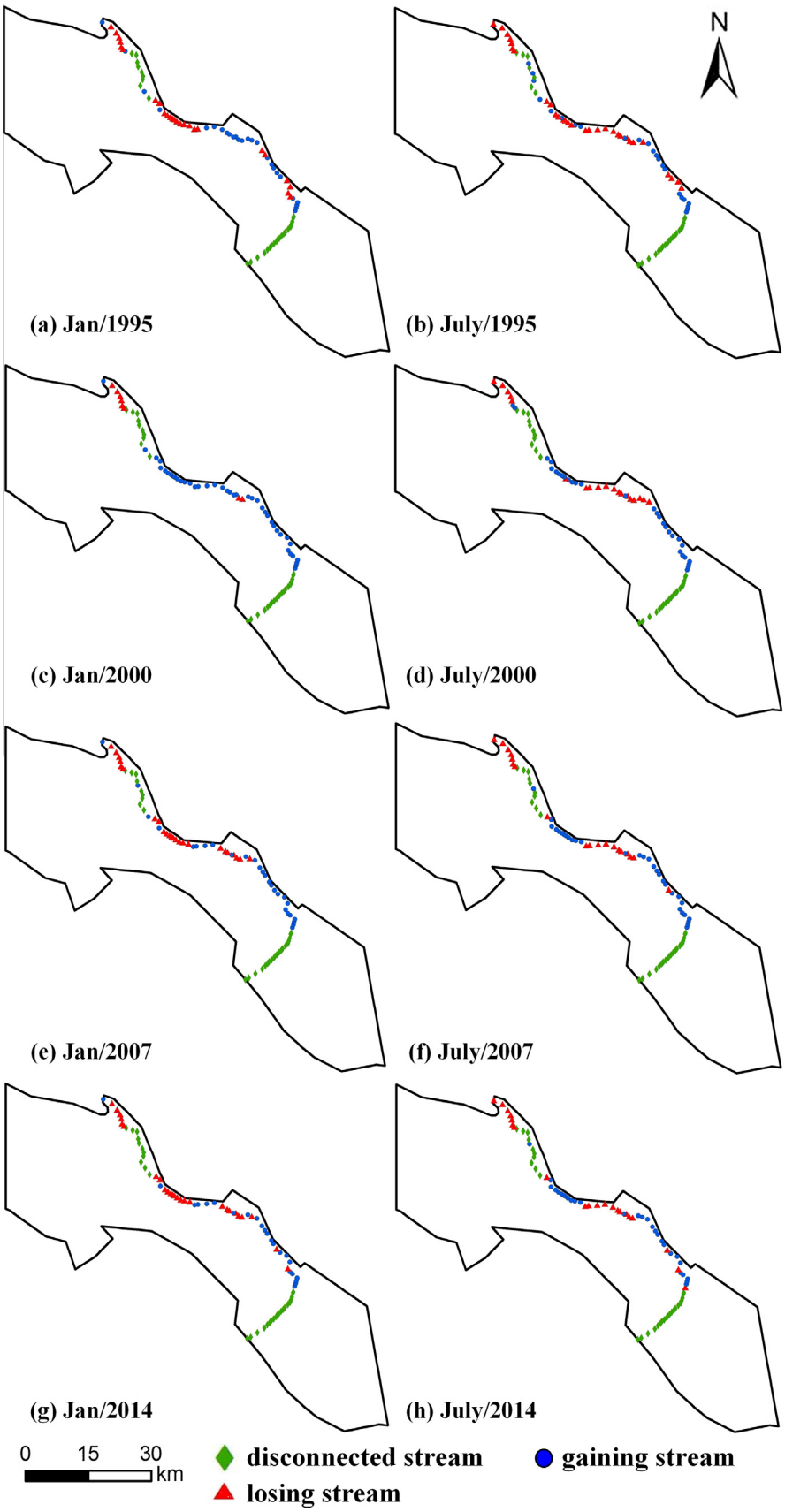

Fig. 8. Changes in the Heihe River-GW relationship.

Please cite this article in press as: Hu, L., et al. Development of a river-groundwater interaction model and its application to a catchment in Northwestern China. J. Hydrol. (2016), http://dx.doi.org/10.1016/j.jhydrol.2016.10.028

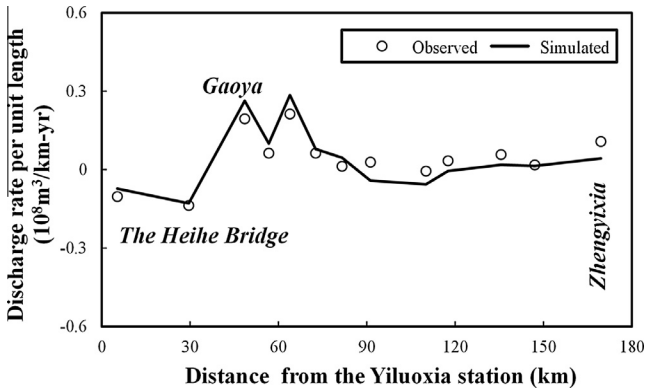

Fig. 9. Comparison of the simulated and observed discharge rates per unit length from the Yiluoxia station in December 2002.

Geological Survey in Gansu Province (Hydrogeoglogical Team and Hydrology and Water Resources Units of Zhangye in Gansu Province, 1990), the total spring flow was approximately 6.29×10^8 m^3 in 1984.

3.3.5. Aquifer parameters

Many aquifer parameters are involved due to the complexity of the aquifer system, including the horizontal and vertical hydraulic conductivities, specific storage, and specific yield. The zones are entirely based on the topography, geology, and soil and rock types. An initial assessment and the possible range of each of the parameters were obtained from various geologic and hydrogeologic reports, pumping test data and previous studies. The infiltration coefficient of precipitation depends on the land use and soil types. A total of 20 zones of hydraulic parameters and 4 zones of infiltration coefficient were defined (Hu et al., 2007).

4. Model calibration and validation

The model calibration period is set from January 1995 to December 2007, and the validation period is set from January 2008 to December 2014. Because the river stage and streamflow data are monthly data, the time step is set to 1 month. To better represent the rapid change of GW levels near pumping wells, the grid cells become progressively finer towards the wells. Details of the mesh system are shown in Fig. 4a, and a cross-section of the model along line BB′ is shown in Fig. 4b. The model includes eight layers, and each layer is represented by 1973 grid cells; thus, the entire model contains 15,784 grid cells. The trial-and-error method and the Fibonacci optimization method (Chen et al., 2014) are both used to calibrate the model against the observed data to achieve the smallest possible objection function, which is defined as the sum of the squares of the differences between the observed and calculated results, including both the water level and spring flux data. Calibrated parameters can be obtained based on previous studies (Hu et al., 2007). During the validation period, data for the observation wells and spring flow are not collected, and so the validation target only includes streamflow of the Heihe River.

4.1. Comparison of observed and simulated data in the open channel model

The simulated streamflow at Gaoya and Zhengyixia agree well with the observed data (Fig. 5a and b). The amplitude of the fluctuation of the simulated streamflow is similar to that of the observed streamflow. Absolute errors of the streamflow of less than 15% are found for approximately 80% of the observed data.

4.2. Comparison of observed and simulated hydraulic heads and spring flows

Six observation wells were chosen from the 34 wells for comparisons between the observed and simulated heads from 1995 to 2007 (Fig. 6a–f). The observed heads in some wells (No. 20, No. 37-1, No. 54, and No. 5.3) show much greater fluctuations than the calculated heads, such as in well No. 37-1. These poor matches may be mainly caused by the fact that due to lack of detailed monthly and spatially distributed data in most irrigation areas, the average GW withdrawals and leakages from channels and irrigated region were assumed to be uniformly allocated to the irrigation areas from June to October. Overall, the trends of the observed and calculated heads are similar, and the peaks are not well consistent, which indicates that the model can accurately simulate the overall trends of the hydrogeological system.

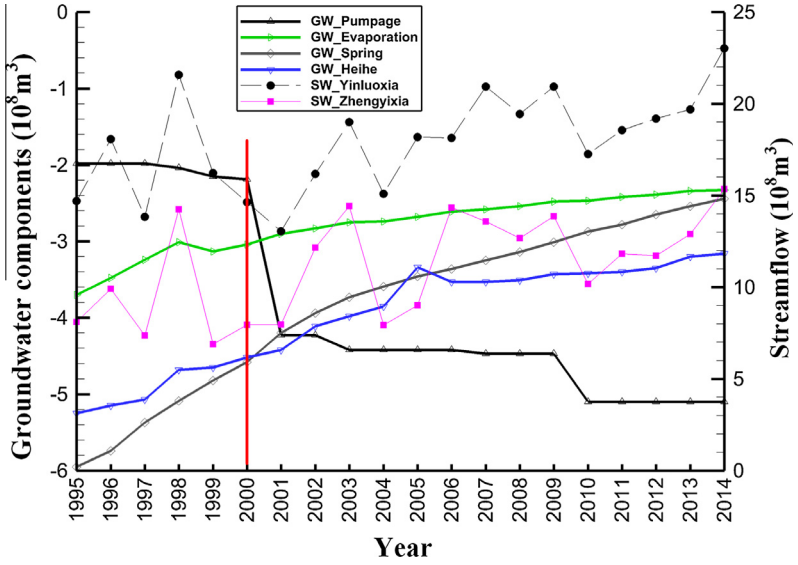

Fig. 10. Simulated results of the GW components and SW streamflow from 1995 to 2014.

Please cite this article in press as: Hu, L., et al. Development of a river-groundwater interaction model and its application to a catchment in Northwestern China. J. Hydrol. (2016), http://dx.doi.org/10.1016/j.jhydrol.2016.10.028

Two springs with long-term observation data are used to calibrate the river-GW model. Fig. 6g and h compare the simulated and observed spring flows at two monitoring sites. The long-term trends for the two springs are similar during the calibration period, but the observed spring flux shows larger fluctuations than the simulated flux (Fig. 6h), mainly because the controlled area of the springs is set to be uniform (Hu et al., 2007).

4.3. Evaluation of model efficiency

To provide information about the overall match between the observed and simulated water levels in all of the monitoring wells, Table 1 presents statistics of the absolute errors in the simulated water levels. The absolute errors in the simulated water level are less than 1 m in more than 65% of the wells. The Nash-Sutcliffe efficiency (NSE) coefficient, which is calculated using Eq. (6), is used to evaluate the model efficiency, including the streamflow at Gaoya and Zhengyixia, the hydraulic heads of all of the observation wells, and the flow rates of two springs

$$E = 1 - \sum_{i=1}^{n}(O_i - P_i)^2 \Big/ \sum_{i=1}^{n}(O_i - \overline{O})^2 \quad (6)$$

where E is the NSE coefficient; n is the total number of data; i is the serial number; O indicates observed data; $\overline{O}$ is the average of all observed data; P indicates simulated values.

Table 2 shows the results of the model efficiency evaluation. The NSE coefficients of the streamflow at Gaoya and Zhengyixia are 0.74 and 0.90, respectively, for the calibration period and 0.75 and 0.96, respectively, for the verification period. The NSE coefficient of the hydraulic heads at the observation wells is 0.99 for the calibration period. However, the NSE coefficient of the spring flow during the calibration period is low (0.21), which is probably because of the uniformly spatial distribution of the GW withdrawals. Overall, the results of the streamflow and hydraulic heads are reasonable because the NSE coefficients of both the streamflow at Zhengyixia and hydraulic heads at all observation wells are over 0.90.

5. Analysis and discussion of the results

5.1. Changes to the water table and its relationship with the Heihe River

Fig. 7 shows simulated contour maps of the water table at the ends of 1995, 2000 and 2007. The maps indicate that the GW flows from the southeast and southwest to the north. As shown in Figs. 2b and 7, groundwater pumpage at the Zhangye city causes significant water table fluctuation (for example, at observation well No. 65 in Fig. 6a) in the upper part of the alluvial fan over the three years, however, small fluctuation is present in the lower part (for example, at observation well No. 37-1 in Fig. 6c).

There are three main types of river-GW relationships (Winter et al., 1998; Brunner et al., 2009) as follows: disconnected streams, connected and gaining streams (denoted as gaining streams), and connected and losing streams (denoted as losing streams). The Heihe River-GW relationship includes all three types and changes between them. The relationship between the Heihe River and GW is time-variant (Fig. 8) and the exchange flux depends on many factors, including hydrogeological parameters (Brunner et al., 2009; Irvine et al., 2012), the river stage and GW level. Overall, the type of river-GW relationship is that of a disconnected stream before the reach at the Heihe Bridge and changes to a gaining stream at Gaoya. In the reaches from Gaoya to Zhengyixia, the relationship may be any of the three stream types. The river-GW relationships change seasonally and are heavily dependent on the water resources and climate conditions from 1995 to 2014. The

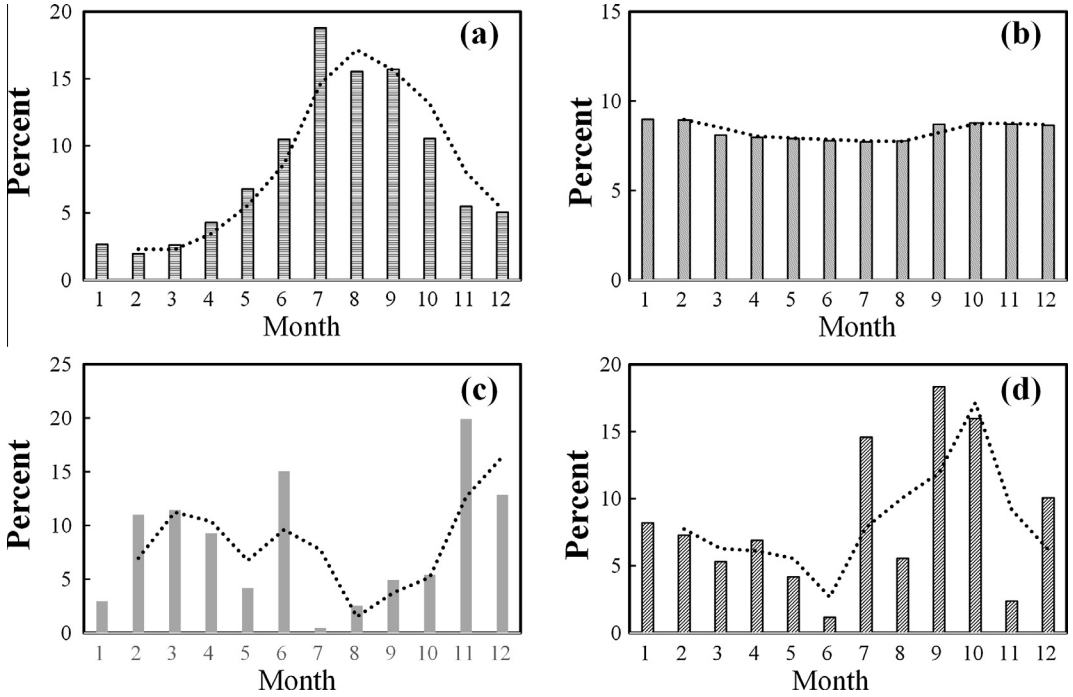

Fig. 11. Monthly average percent streamflow at Yiluoxia (a), GW discharge to springs (b) and the Heihe River (c), and streamflow at Zhengyixia (d) from 1995 to 2014 (dashed lines indicate the trends of the changes).

GW levels tended to recover from 1995 to 2000 and then were depleted from 2000 to 2014, which is mainly because the GW pumpage is greatly increased. The relationship in some sections of the Heihe River changed from a gaining stream in January to a losing stream or disconnected stream in July.

5.2. Changes of the Heihe River-groundwater relationship

The simulated annual GW discharge to the Heihe River and springs decreases slightly every year because the relationship between the Heihe River and the GW is largely controlled by the water table in the lower reaches of the Heihe River, which is affected by the amount of GW exploitation. The model results show that the average annual amount of water lost from the Heihe River from Yinluoxia to the Heihe Bridge between 1995 and 2014 is approximately 2.50×10^8 m^3, which accounts for 17% of the annual average streamflow at Yinluoxia (15.80×10^8 m^3). The GW may discharge directly to the Heihe River or discharge to springs and then flow into the main stream indirectly. The simulated results demonstrate that direct GW and indirect discharges to the Heihe River is approximately 7.80×10^8 m^3 (more than 49% of the mean streamflow at Yinluoxia).

To further analyse the Heihe River-GW interaction, the simulated yearly average discharge rate per unit length from Yiluoxia in December 2002 is shown in Fig. 9 and is compared with the results of a field investigation by the Zhangye Provincial Bureau of Hydrological and Water Resources Survey. The simulated results and observations agree relatively well. The negative values in Fig. 9 indicated that the Heihe River is a disconnected or losing stream, and the positive values indicate that the Heihe River is a gaining stream. The lowest point in the curves in Fig. 9 is located at the Heihe Bridge, and the high peak is near Gaoya, which indicates that the river-GW relationship changes from a disconnected stream in the reaches before the Heihe Bridge to a gaining stream or losing stream after the Heihe Bridge.

5.3. Water balance analysis of the SW-GW interaction

The main GW recharge sources are rivers, channel seepage, and return flows of irrigation water. Water balance of the river-GW interaction based on the simulation from 1995 to 2014 are made. The annual mean SW infiltration, irrigation water infiltration and return flow is more than 10.00×10^8 m^3, which represents more than 94% of the total GW recharge. The main GW discharge components are derived from rivers, springs, GW evaporation, and GW abstraction. The annual mean GW evaporation is approximately 2.78×10^8 m^3, and the annual mean GW pumpage is approximately 3.87×10^8 m^3. The annual mean GW discharge to the Heihe River and springs is more than 7.80×10^8 m^3, which represents approximately 54% of the total GW discharge.

5.4. Inter-annual and intra-annual river-GW relationships

Fig. 10 shows the simulated results of the changes of the GW components and the streamflow of the Heihe River from 1995 to 2014. GW evaporation and GW discharges to springs and the Heihe River decrease every year. However, the streamflow of the Heihe River at Zhengyixia has a similar increasing trend as that at Yinluoxia. The changes of GW and streamflow at Zhengyixia shown in Fig. 10 were mainly caused by the implementation of the water reallocation plan for the Heihe River in 2000, the overexploitation of GW for agriculture water use and streamflow at Yinluoxia. The streamflow of the Heihe River at Zhengyixia is not significantly affected by the increase of GW abstraction, which may be caused by the change in the river-GW relationship from a gaining stream to a losing stream in some reaches. The degradation of the river-GW relationship from a gaining stream to a losing stream or a disconnected stream indicates that GW pumpage in the middle reaches should be rationally controlled to sustain the natural water balance of the GW system.

In addition, the monthly average percentages of streamflow and GW discharge have different variations. The mean intra-annual streamflow at Zhengyixia is significantly different from that at Yinluoxia (Fig. 11a and d). The annual mean streamflow at Zhengyixia peaks around October, while the peak streamflow at Yinluoxia occurs in July, which suggests that the peak streamflow has a time lag effect. The annual mean direct GW discharge to the Heihe River (Fig. 11c) varies significantly over the year and has a peak in the winter (November-December). The annual mean GW discharge to the springs (Fig. 11b) has a small variation and a peak in the winter (November-December).

6. Conclusions

In the middle and lower reaches of river basins of most arid regions, the process of precipitation-runoff is not significant, however, water consumption and streamflow are dominant processes. Accordingly, a coupled river-GW model is developed to describe the dynamic river-GW relationship and conversion at the basin scale as well as groundwater flow and streamflow. An example of the data collection, model construction and model calibration is given to discuss temporal-spatial change of river-groundwater relationships under human activities in recent years. The coupled river-GW model includes a one-dimensional open channel flow model and a three-dimensional saturated GW flow model. The model is tested with three benchmark cases as follows: the problem of a continuous point sink in a homogeneous aquifer, the channel flow problem of the Sacramento River and the river-GW relationship induced by GW pumping. The good agreement between the simulated and analytical or observed values demonstrates that the model can provide reasonable results of the river-GW interactions. Due to the representative and complicated river-GW interactions in the HRB, an externally coupled river-GW model of the middle reaches is developed. Compared with traditional saturated GW flow models, the coupled model of the middle reaches of the HRB can simulate the river stage, streamflow, hydraulic head and spring flow at much higher spatial and temporal resolutions. The integrated river-GW model is calibrated and validated with the most up-to-date hydrologic and hydrogeologic data in the HRB from 1995 to 2014. The calibration targets include the hydraulic heads of 34 observation wells, streamflow, spring flow and field investigations of the river-GW conversion. After the calibration and validation, the integrated model is used to analyse the trends of the changes of the GW system and the open channel, which can be used to analyse water resource management under different water use strategies in irrigation areas.

The river-GW relationships in the HRB change spatially and seasonally and are well demonstrated by the developed model. The results show that the annual mean loss of water from the Heihe River from Yinluoxia to the Heihe Bridge is approximately 2.50×10^8 m^3, and the direct and indirect GW discharges to the Heihe River are approximately 7.80×10^8 m^3. Simulations also found that after the implementation of the water resources reallocation plan of the HRB, increment in groundwater pumpage causes the change of the river-GW relationship from a gaining stream to a losing stream or a disconnected stream.

This study mainly addresses the river-GW relationship under water use and climate conditions, which will enhance the understanding of the river-GW relationship in the middle reaches of the HRB. Because the amount and spatial and temporal distribution of GW pumpage in each irrigation area are difficult to achieve, GW

Please cite this article in press as: Hu, L., et al. Development of a river-groundwater interaction model and its application to a catchment in Northwestern China. J. Hydrol. (2016), http://dx.doi.org/10.1016/j.jhydrol.2016.10.028

pumpage data in low spatial and temporal resolutions causes poor performance of the simulated hydraulic head at some observation wells. Only yearly streamflow data of the Heihe River from the year of 2008–2014 is collected and the monthly allocation of streamflow during this period remains the same for each year. No parameter sensitivity analyses are carried out, and further investigations, such as temporo-spatially distributed groundwater pumpage, are still needed to refine data input. At the basin scale, a complicated model that couples SW, GW, ecology and society is highly urged to optimize the uses of SW and GW and keep the balance among water use, economy and ecology, which is our ongoing work.

Acknowledgements

This study was supported by the National Natural Science Foundation of China (grant numbers 91125015 and 41572220) and the Research and Development Project on Geological Disposal of High Level Radioactive Waste by the State Administration of Science, Technology and Industry for National Defense (grant number 2012-240). The authors also express their thanks to the Zhangye Provincial Bureau of Hydrological and Water Resources Survey, the Hydrogeological Team and Hydrology and Water Resources Units of Zhangye in Gansu Province, China, which provided information about the site hydrogeology and groundwater and river data. In addition, some data were provided by the Cold and Arid Regions Science Data Center in Lanzhou, China (http://westdc.westgis.ac.cn). We also appreciate the constructive comments and suggestions from five anonymous reviewers.

Appendix A. Test cases

A.1. Problem of a continuous point sink in a homogenous aquifer

The drawdown in an open and infinite aquifer with a continuous point sink with zero penetration length located at the top of the aquifer can be expressed as Eq. (A1) (Carslaw, 1921; Chen, 1966)

$$s = \frac{Q_p}{4\pi K_p \rho} erfc\left(\frac{\rho}{2\sqrt{K_p t/S_s}}\right) \quad \text{(A1)}$$

where s is the drawdown at (x, y, z) (L); Q_p is the pumping rate (L^3/T); K_p is the hydraulic conductivity (L/T); ρ is the distance from the observation point to the pumping well ($\rho = \sqrt{x^2 + y^2 + z^2}$) (L); S_s is the specific storage (1/L); t is the time since the beginning of pumping (L); and *erfc* is the complementary error function.

Assume $K_p = 100$ m/d, $S_s = 10^{-6}$ m^{-1}, and $Q_p = 100$ m^3/d. The model domain is 868,146.5 m by 868,146.5 m. The pumping well is placed at the centre of the domain. To better describe the rapid change of the water level near the pumping well, the grid cells become progressively finer towards the pumping well. This design of the model domain ensures that the boundary condition has a negligible impact on the drawdown calculated near the well for a given pumping duration. Vertically, the aquifer is divided into 21 model layers. The first and last layers are 2.5 m thick, and the other layers are 5.0 m thick. To minimize the error caused by the numerical calculation, the convergence criterion of each grid cell is set to 0.0001 m. The drawdown induced by pumping will change rapidly in the first several days, and the magnitude of the drawdown will then decrease. The simulation time is set to 10.3 days with 127 time steps, an initial time step of 0.001 days and a time step expansion factor of 1.05. The changes of drawdown with the radial distance in the top layer, the middle layer and the bottom layer for the entire aquifer are shown in Fig. A1a, b and c, respectively.

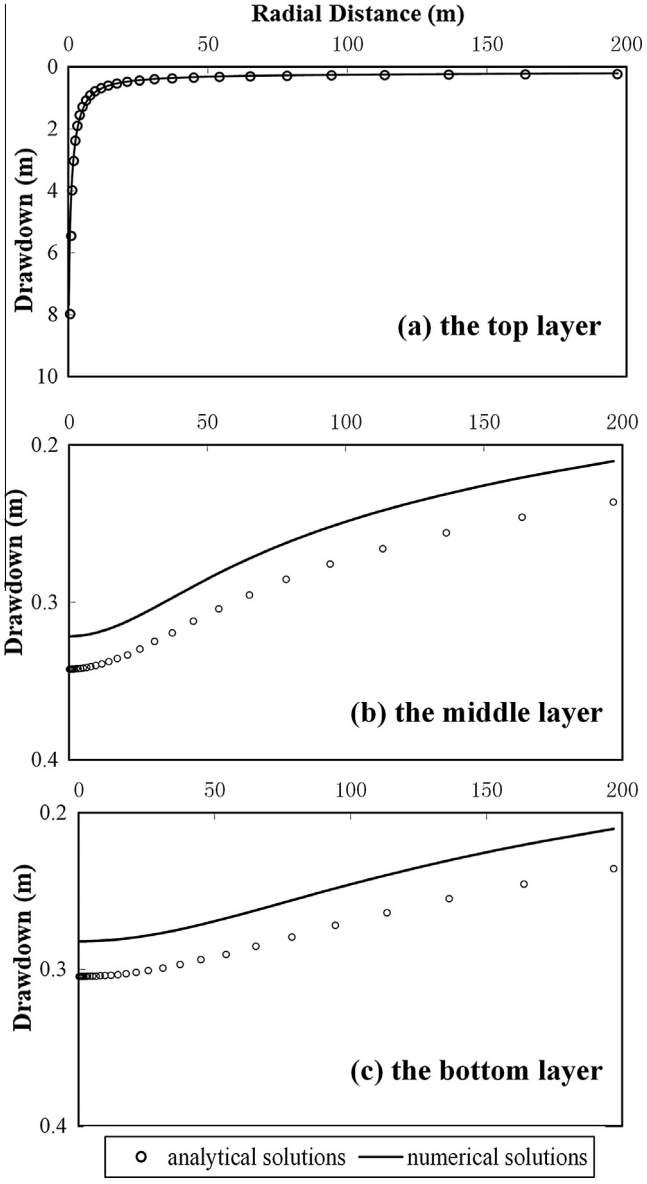

Fig. A1. Comparisons between the analytical and numerical solutions for a continuous point sink problem. (a) Top layer; (b) middle layer and (c) bottom layer.

The results show that the matches between the numerical and analytical solutions are nearly perfect.

A.2. Channel flow problem of the Sacramento River

The Sacramento River (Schaffranek et al., 1981) is selected as a case study to illustrate the application of the open channel flow model. The Sacramento River is a tide-affected reach that extends downstream from the city of Sacramento to near the town of Freeport, Calif (Fig. A2). Two hydrological stations (A and B) are located along this reach, which is approximately 17.4 km long and is selected as the model area. The river stages at the two hydrological stations are known. When the initial river stage and streamflow are given, the streamflow of the reach between A and B can be simulated. A flow-resistance coefficient (η, $\eta = k^{0.5}$) is expressed in terms of a quadratic function of the discharge. The functional relationship is determined as in previous studies (Schaffranek et al., 1981). Fig. A3 shows a comparison between the observed and sim-

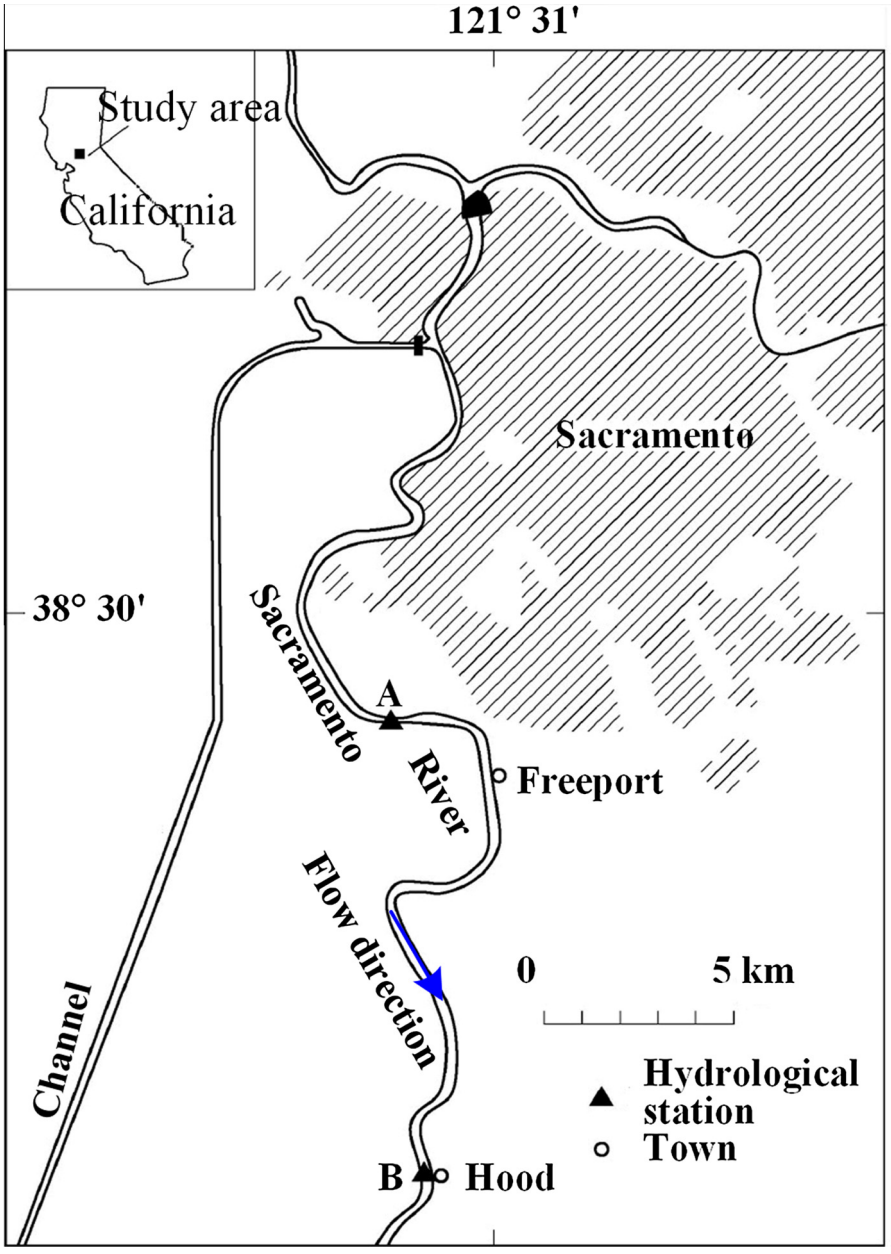

Fig. A2. Schematic map of the Sacramento River channel flow problem.

ulated streamflow at hydrological station A. The simulated streamflow agrees well with the observed values.

A.3. Change of the river-groundwater relationship induced by groundwater pumping

This hypothetical case is used to illustrate the change of the simulated river-GW relationship induced by GW pumping. The domain is set to be 2000 m wide and 500 m long (Fig. A4a). The aquifer is assumed to be homogeneous with a horizontal impermeable layer. The river is located in the middle of the study area. The aquifer is 100 m thick except for near the river, where it is 10 m thick. The annual rainfall is assumed to be 600 mm, and the recharge coefficient of rainfall is set as 0.1. The river stage is constant and remains at 10 m. The flux conductivity of the river-GW interaction is set as 41.67 m^2/d. The bottom elevation of the impermeable layer under the river is 9.5 m. The hydraulic conductivity is 15 m/d, and the specific yield is set as 0.1. The GW system is

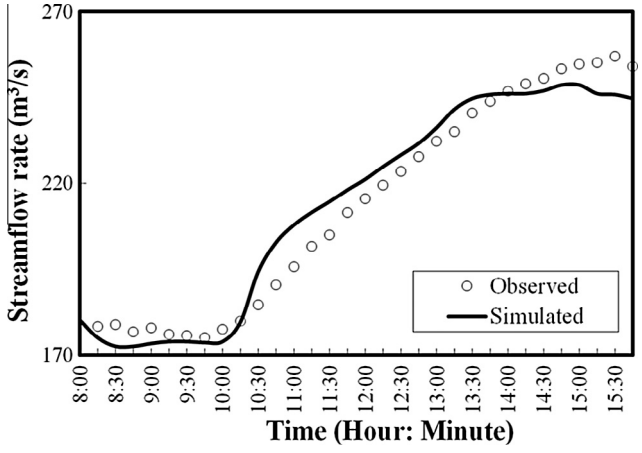

Fig. A3. Comparison between the observed and simulated streamflow at hydrological station A.

Please cite this article in press as: Hu, L., et al. Development of a river-groundwater interaction model and its application to a catchment in Northwestern China. J. Hydrol. (2016), http://dx.doi.org/10.1016/j.jhydrol.2016.10.028

assumed to be at steady state before pumping begins. When GW pumping at two wells (W1 and W2) begins, the river-GW relationship will change. The coordinates of the first and second pumping wells are (−100, 0) and (100, 0), respectively. The pumping rate of the two wells is 500 m^3/d. The initial time step is set as 0.5 days, and the total number of time steps is set as 1000. The model contains 601 polygonal grid cells (Fig. A4b).

Fig. A5 shows the changes of the simulated water table after 3 days, 26.5 days, and 500 days. The greatest drawdown is near the pumping wells. At the beginning of GW pumping, the water table is over 10 m, which verified that the river is a gaining stream. The water table decreases with time. After 3 days, the water table is below 9.5 m in only a small area near the pumping well, and thus the relationship has changed to a losing stream and a disconnected

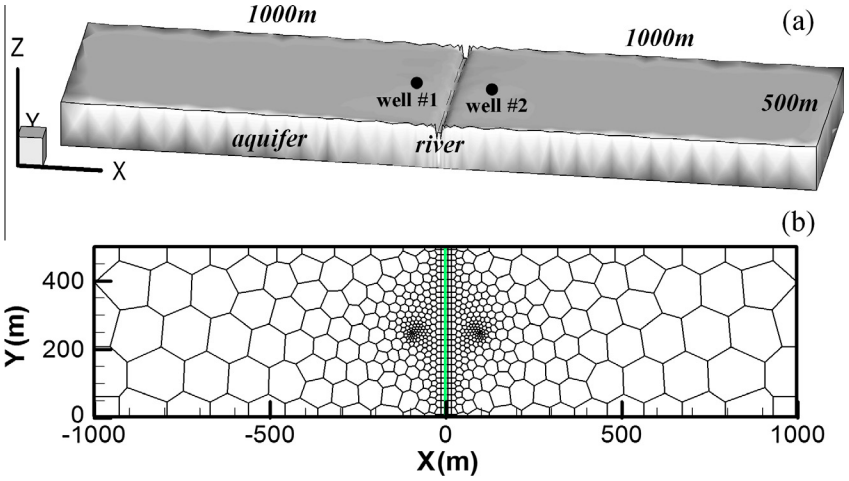

Fig. A4. Schematics of the coupled river-GW model induced by GW pumping. (a) Model area and (b) model mesh in plane view.

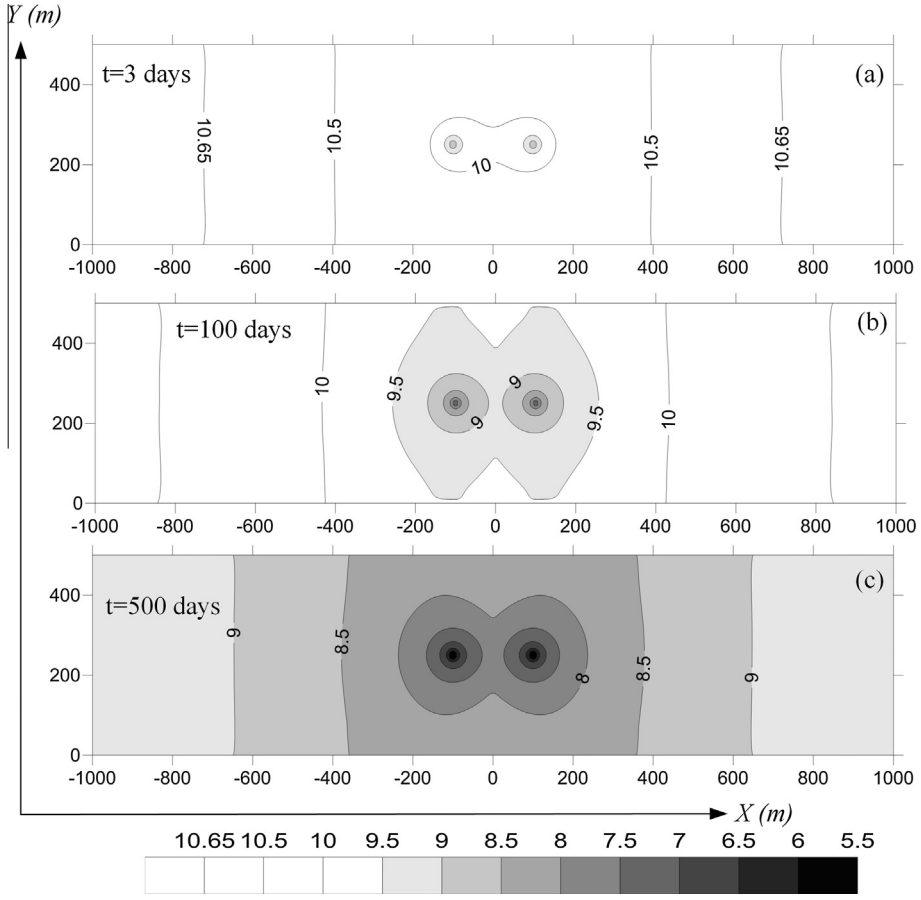

Fig. A5. Contour maps of the GW level after 3 days (a), 100 days (b) and 500 days (c).

Please cite this article in press as: Hu, L., et al. Development of a river-groundwater interaction model and its application to a catchment in Northwestern China. J. Hydrol. (2016), http://dx.doi.org/10.1016/j.jhydrol.2016.10.028

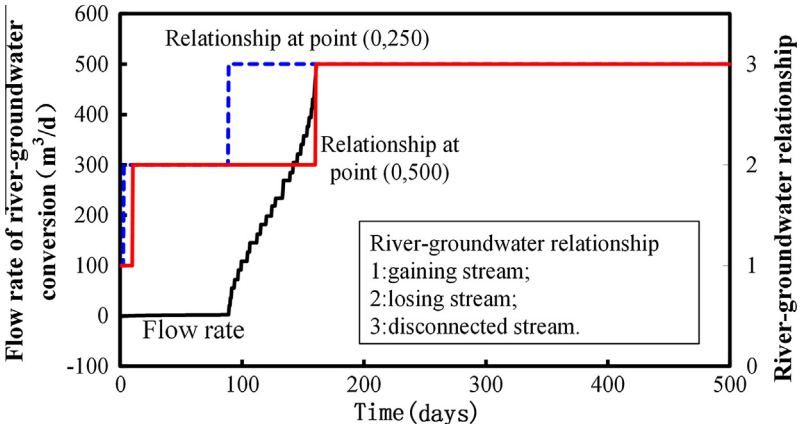

Fig. A6. Changes of the exchange flow rate and the relationship between the river and GW with time.

stream. After 26.5 days, the area where the water table is below 9.5 m has increased significantly. After 500 days, most of the domain has changed to a disconnected stream. Fig. A6 shows the change of the river–groundwater flux exchange and the evolution of the river-GW relationship with time. Using the point (0, 500) as an example, the river-GW interaction is initially a gaining stream, changes to a losing stream at approximately 10 days, and finally becomes a disconnected stream at 185 days. The river–groundwater flux exchange increases with time and peaks at 185 days.

References

Abel, B.A., Loague, K., Montgomery, D.R., Dietrich, W.E., 2008. Physics-based continuous simulation of long-term near-surface hydrologic response for the Coss Bay experimental catchment. Water Resour. Res. 44 (7), W07417. http://dx.doi.org/10.1029/2007WR006442.

Brunner, P., Cook, P.G., Simmons, C.T., 2009. Hydrogeologic controls on disconnection between surface water and groundwater. Water Resour. Res. 45, W01422. http://dx.doi.org/10.1029/2008WR006953.

Carslaw, H.S., 1921. Introduction to the Mathematical Theory of the Conduction of Heat in Solids. Macmillan and Co. Limited, London, p. 268. Completely Revised, P149–151.

Chen, C.X., 1966. Groundwater Hydraulics. Beijing Geology College, Beijing, China (in Chinese).

Chen, C.X., 1998. "Hysteresis recharge weight function" method: for solving the rainfall hysteretic recharge to the water table. Hydrogeol. Eng. Geol. 25 (6), 22–24 (in Chinese With English abstract).

Chen, C.X., Pei, S.P., Jiao, J.J., 2003. Land subsidence caused by groundwater exploitation in Suzhou City, China. Hydrogeol. J. 11 (2), 275–287.

Chen, C.X., Tang, Z.H., Hu, L.T., 2014. Numerical Methods and Model Design of Groundwater Flow Problem. Geological publishing house, Beijing, China (in Chinese).

Chen, X.H., Burbach, M., Cheng, C., 2008. Electrical and hydraulic vertical variability in channel sediments and its effects on streamflow depletion due to groundwater extraction. J. Hydrol. 352 (3–4), 250–266.

Cheng, G.D., Li, X., Zhao, W.Z., Xu, Z.M., Feng, Q., Xiao, S.C., Xiao, H.L., 2014. Integrated study of the water–ecosystem–economy in the Heihe River Basin. Natl. Sci. Rev. 1 (3), 413–428.

Deng, X.Z., Zhao, C.H., 2015. Identification of water scarcity and providing solutions for adapting to climate changes in the Heihe River Basin of China. Adv. Meteorol. 279173. http://dx.doi.org/10.1155/2015/279173.

Fernald, A.G., Guldan, S.J., 2006. Surface water–groundwater interactions between irrigation ditches, alluvial aquifers, and streams. Rev. Fish. Sci. 14 (1), 79–89.

Furman, A., 2008. Modeling coupled surface-subsurface flow processes: a review. Vadose Zone J. 7 (2), 741–756.

Harvey, J.W., Newlin, J.T., Krupa, S.L., 2006. Modeling decadal timescale interactions between surface water and ground water in the central Everglades, Florida, USA. J. Hydrol. 320 (3–4), 400–420.

Hu, L.T., Chen, C.X., Jiao, J.J., Wang, Z.J., 2007. Simulated groundwater interaction with rivers and springs in the Heihe river basin. Hydrol. Process. 21 (20), 2794–2806.

Hu, L.T., Wang, Z.J., Tian, W., Zhao, J.S., 2009. Coupled surface water-groundwater model and its application in the arid Shiyang River basin, China. Hydrol. Process. 23 (14), 2033–2044.

Hu, L.T., Zhang, K., Cao, X.Y., Li, Y., Guo, C.B., 2016. IGMESH: a convenient irregular-grid-based pre- and post- processing tool for TOUGH2 simulator. Comput. Geosci. 95, 11–17.

Hui, F.M., Yin, Y.Y., Qi, J.G., Gong, P., 2005. Land degradation in the Heihe River Basin in relation to plant growth conditions. Geogr. Inform. Sci. 11 (2), 147–154.

Hydrogeological Team and Hydrology and Water Resources Units of Zhangye in Gansu Province, 1996. Soil moisture movement and its water balance analysis in the middle reaches of the Heihe River Basin, Gansu, China, Unpublished Report (in Chinese).

Hydrogeological Team and Hydrology and Water Resources Units of Zhangye in Gansu Province, 1990. Investigation on rational groundwater resources exploitation in the middle reaches of the Heihe River Basin, Gansu, China, Unpublished Report (in Chinese).

Irvine, D.J., Brunner, P., Franssen, H.-J.H., Simmons, C.T., 2012. Heterogeneous or homogeneous? Implications of simplifying heterogeneous streambeds in models of losing streams. J. Hydrol. 424, 16–23.

Jia, Y.W., Ding, X., Qin, C., et al., 2009. Distributed modeling of land surface water and energy budgets in the inland Heihe River Basin of China. Hydrol. Earth Syst. Sci. 13, 1849–1866.

Katz, B.G., Coplen, T.B., Bullen, T.D., Davis, J.H., 1997. Use of chemical and isotopic tracers to characterize the interactions between ground water and surface water in mantled karst. Ground Water 35 (6), 1014–1028.

Kumar, U.S., Sharma, S., Navada, S.V.M., 2008. Recent studies on surface water–groundwater relationships at hydro-projects in India using environmental isotopes. Hydrol. Process. 22 (23), 4543–4553.

Lamontagne, S., Leaney, F.W., Herczeg, A.L., 2005. Groundwater-surface water interactions in a large semi-arid floodplain: implications for salinity management. Hydrol. Process. 19 (16), 3063–3080.

Lan, Y.C., Kang, E.S., Zhang, J.S., et al., 2002. Study on the mutual transformation between groundwater and surface water resources in the Hexi inland arid regions. Adv. Earth Sci. 17 (4), 535–545.

Lang, Y.C., Liu, C.Q., Zhao, Z.Q., 2006. Geochemistry of surface and ground water in Guiyang, China: water/rock interaction and pollution in a karst hydrological system. Appl. Geochem. 21 (6), 887–903.

Malcolm, I.A., Soulsby, C., Youngson, A.F., Petry, J., 2003. Heterogeneity in ground water-surface water interactions in the hyporheic zone of a salmonid spawning stream. Hydrol. Process. 17 (3), 601–617.

Markstrom, S.L., Niswonger, R.G., Regan, R.S., Prudic, D.E., Barlow, P.M., 2008. GSFLOW-coupled ground-water and surface-water flow model based on the integration of the Precipitation-Runoff Modeling System (PRMS) and the Modular Ground-Water Flow Model (MODFLOW-2005). USGS Techniques and Methods, 6-D1, 240 pp.

Miller, S.A., Johnson, G.S., Cosgrove, D.M., Larson, R., 2003. Regional scale modeling of surface and ground water interaction in the Snake River Basin. J. Am. Water Resour. Assoc. 39 (3), 517–528.

Neville, C.J., Tonkin, M.J., 2004. Modeling multiaquifer wells with MODFLOW. Ground Water 42 (6), 910–919.

Newman, B.D., Vivoni, E.R., Groffman, A.R., 2006. Surface water-groundwater interactions in semiarid drainages of the American southwest. Hydrol. Process. 20 (15), 3371–3394.

Nian, Y.Y., Li, X., Zhou, J., Hu, X.L., 2014. Impact of land use change on water resource allocation in the middle reaches of the Heihe River Basin in northwestern China. J. Arid Land 6 (3), 273–286.

Ojiambo, B.S., Poreda, R.J., Lyons, W.B., 2001. Ground water/surface water interactions in Lake Naivasha, Kenya, using delta O-18, delta D, and H-3/He-3 age-dating. Ground Water 39 (4), 526–533.

Panday, S., Huyakorn, P.S., 2004. A fully coupled physically-based spatially-distributed model for evaluating surface/subsurface flow. Adv. Water Resour. 27 (4), 361–382.

Partington, D., Brunner, P., Simmons, C.T., Werner, A.D., Therrien, R., Maier, H.R., Dandy, G.C., 2012. Evaluation of outputs from automated baseflow separation methods against simulated baseflow from a physically based, surface water-groundwater flow model. J. Hydrol. 458, 28–39.

Pucci, A.A., Pope, D.A., 1995. Simulated effects of development on regional ground-water/surface-water interactions in the Northern coastal-plain OF New-Jersey. J. Hydrol. 167 (1–4), 241–262.

Refsgaard, J.C., 1997. Parameterization, calibration and validation of distributed hydrological models. J. Hydrol. 198 (1–4), 69–97.
Schaffranek, R.W., Baltzer, R.A., Goldberg, D.E., 1981. A Model for Simulation of Flow in Singular and Interconnected Channels. U.S. Geological Survey Techniques of Water Resources Investigations, p. 110 (Book 7, Chap.C3).
Sophocleous, M., 2002. Interactions between groundwater and surface water: the state of the science. Hydrogeol. J. 10 (1), 52–67.
Swain, E.D., Wexler, E.J., 1996. A Coupled Surface-Water and Groundwater Flow Model (MODBRNCH) for Simulation of Stream-Aquifer Interaction. Techniques of Water-Resources Investigations of the United States Geological Survey, Washington, DC, p. 125 (Book 6, Chap. A6).
Therrien, R., McLaren, R.G., Sudicky, E.A., 2007. HydroGeoSphere—A Three-Dimensional Numerical Model Describing Fully-Integrated Subsurface and Surface Flow and Solute Transport. Groundwater Simulations Group, University of Waterloo.
Tian, Y., Zheng, Y., Wu, B., Wu, X., Liu, J., Zheng, C.M., 2015a. Modeling surface water-groundwater interaction in arid and semi-arid regions with intensive agriculture. Environ. Model. Software 63, 170–184.
Tian, Y., Zheng, Y., Zheng, C.M., Xiao, H.L., Fan, W.J., Zou, S.B., Wu, B., Yao, Y.Y., Zhang, A.J., Liu, J., 2015b. Exploring scale dependent ecohydrological responses in a large endorheic river basin through integrated surface water groundwater modeling. Water Resour. Res. 51. http://dx.doi.org/10.1002/2015WR016881.
Velazquez, M.P., Andreu, J., Sahuquillo, A., Velazquez, D.P., 2008. Hydro-economic river basin modelling: the application of a holistic surface-groundwater model to assess opportunity costs of water use in Spain. Ecol. Econ. 66 (1), 51–65.
Wang, W.K., Li, J.T., Feng, X.Z., Chen, X.H., Yao, K.J., 2011. Evolution of stream-aquifer hydrologic connectedness during pumping—experiment. J. Hydrol. 402 (3–4), 401–414.
Wang, X.J., Yang, H., Shi, M.J., Zhou, D.Y., Zhang, Z.Y., 2015. Managing stakeholders' conflicts for water reallocation from agriculture to industry in the Heihe River Basin in Northwest China. Sci. Total Environ. 505, 823–832.
Wang, X.S., Ma, M.G., Li, X., Zhao, J., Dong, P., Zhou, J., 2010. Groundwater response to leakage of surface water through a thick vadose zone in the middle reaches area of Heihe River Basin, China. Hydrol. Earth Syst. Sci. 14 (4), 639–650.
Wang, Z.J., Zhu, J.F., Zheng, H., 2015. Improvement of duration-based water rights management with optimal water intake on/off events. Water Resour. Manage 29 (8), 2927–2945.
Ward, A.S., Payn, R.A., Gooseff, M.N., McGlynn, B.L., Bencala, K.E., Kelleher, C.A., Wondzell, S.M., Wagener, T., 2013. Variations in surface water-ground water interactions along a headwater mountain stream: comparisons between transient storage and water balance analyses. Water Resour. Res. 49 (6), 3359–3374.
Werner, A.D., Gallagher, M.R., Weeks, S.W., 2006. Regional-scale, fully coupled modelling of stream-aquifer interaction in a tropical catchment. J. Hydrol. 328 (3–4), 497–510.
Winter, T.C., 1995. Recent advances in understanding the interaction of groundwater and surface water. Rev. Geophys. 33 (Suppl.), 985–994.
Winter, T.C., Harvey, J.W., Franke, O.L., Alley, W.M., 1998. Ground water and surface water – a single resource. U.S. Geological Survey Circular 1139, 79 pp.
Woocay, A., Walton, J., 2008. Multivariate analyses of water chemistry: surface and ground water interactions. Ground Water 46 (3), 437–449.
Wu, B., Zheng, Y., Wu, X., Tian, Y., Han, F., Liu, J., Zheng, C.M., 2015. Optimizing water resources management in large river basins with integrated surface water-groundwater modeling: a surrogate-based approach. Water Resour. Res. 51, 2153–2173. http://dx.doi.org/10.1002/2014WR016653.
Wu, D.D., Anagnostou, E.N., Wang, G.L., Moges, S., Zampieri, M., 2014. Improving the surface-ground water interactions in the community land model: case study in the Blue Nile Basin. Water Resour. Res. 50 (10), 8015–8033.
Wu, X.J., Zhou, J., Wang, H.J., Li, Y., Zhong, B., 2015. Evaluation of irrigation water use efficiency using remote sensing in the middle reach of the Heihe river, in the semi-arid Northwestern China. Hydrol. Process. 29 (9), 2243–2257.
Yao, Y.Y., Zheng, C.M., Liu, J., Cao, G.L., Xiao, H.L., Li, H.T., Li, W.P., 2015a. Conceptual and numerical models for groundwater flow in an arid inland river basin. Hydrol. Process. 29 (6), 1480–1492.
Yao, Y.Y., Zheng, C.M., Tian, Y., Liu, J., Zhen, Y., 2015b. Numerical modeling of regional groundwater flow in the Heihe River Basin, China: advances and new insights. Sci. China: Earth Sci. 58 (1), 3–15.
Yu, Z.B., Schwartz, F.W., 1998. Application of an integrated basin-scale hydrologic model to simulate surface-water and ground-water interactions. J. Am. Water Resour. Assoc. 34 (2), 409–425.
Yuan, D., Lin, B.L., 2009. Modelling coastal ground- and surface-water interactions using an integrated approach. Hydrol. Process. 23 (19), 2804–2817.
Zaadnoordijk, W.J., 2009. Simulating piecewise-linear surface water and ground water interactions with MODFLOW. Ground Water 47 (5), 723–726.
Zhang, A.J., Liu, J., 2015. Exploring scale dependent ecohydrological responses in a large endorheic river basin through integrated surface water groundwater modeling. Water Resour. Res. 51. http://dx.doi.org/10.1002/2015WR016881.
Zhong, G.Q., 1995. The History Book of Ancient Zhangye City. Gansu Culture Press, Lanzhou, China (in Chinese).
Zhu, F.F., Huang, W.R., Cai, Y., Teng, F., Wang, B.B., Zhou, Q., 2014. Development of a river hydrodynamic model for studying surface-ground water interactions affected by climate change in Heihe River, China. J. Coastal Res. S68, 129–135.

Please cite this article in press as: Hu, L., et al. Development of a river-groundwater interaction model and its application to a catchment in Northwestern China. J. Hydrol. (2016), http://dx.doi.org/10.1016/j.jhydrol.2016.10.028